Advanced Concepts for Dry Storage Cask Thermal-Hydraulic Testing

Spent Fuel and Waste Disposition

Sandia National Laboratories

ABSTRACT

The purpose of this report is to review technical issues relevant to the performance evaluation of dry storage systems during vacuum drying and long-term storage operations. It also provides updates on experimental components under development that are vital for pursuing advanced studies. Validation of the extent of water removal in a multi-assembly dry storage system using an industrial vacuum drying procedure is needed, as operational conditions leading to incomplete drying may have potential impacts on the fuel, cladding, and other components in the system. Water remaining in canisters/casks upon completion of vacuum drying can lead to cladding corrosion, embrittlement, and breaching, as well as fuel degradation. Therefore, additional information is needed to evaluate the potential impacts of water retention on extended long-term dry storage. A general lack of data and experience modeling the drying process necessitates the testing of advanced concepts focused on the simulation of industrial vacuum drying. Smaller-scale tests that incorporate relevant physics and well-controlled boundary conditions are necessary to provide insight and guidance to the modeling of prototypic systems undergoing drying processes.

This report describes the development and testing of waterproof, electrically-heated spent fuel rod simulators as a proof of concept to enable experimental simulation of the entire dewatering and drying process. This report also describes the preliminary development of specially-designed, unheated mock fuel rods for monitoring internal rod pressures and studying water removal from simulated failed fuel rods. A variety of moisture monitoring instrumentation is also being considered and will be downselected for the tracking of dewpoints of gas samples. The effects of cladding oxidation and crud on water retention in dry storage systems can be explored via separate effects tests (SETs) that would measure chemisorbed and physisorbed water content on cladding samples. The concepts listed above will be incorporated into an advanced dry cask simulator with multiple fuel assemblies in order to account for important inter-assembly heat-transfer physics. Plans are described for harvesting up to five full-length 5×5 laterally truncated assemblies from commercial 17×17 PWR skeleton components with the goal of constructing this simulator.

This page is intentionally left blank.

ACKNOWLEDGEMENTS

This page is intentionally left blank.

CONTENTS

LIST OF FIGURES

This page is intentionally left blank.

LIST OF TABLES

This page is intentionally left blank.

ACRONYMS / ABBREVIATIONS

BWR	boiling water reactor
CFD	computational fluid dynamics
CNWRA	Center for Nuclear Waste Regulatory Analyses
DAQ	data acquisition system
DCS	Dry Cask Simulator
DOE	Department of Energy
EPRI	Electric Power Research Institute
FHD	forced helium dehydration
HBU	high burnup
MAWP	maximum allowable working pressure
MS	mass spectroscopy
NE	nuclear energy
NEUP	Nuclear Energy University Program
NRC	Nuclear Regulatory Commission
PCT	peak cladding temperature
PRV	pressure relief valve
PT	pressure transducer
PWR	pressurized water reactor
SCR	silicon-controlled rectifier
SET	separate effects test
SFWD	Spent Fuel and Waste Disposition Campaign
SNF	spent nuclear fuel
SS	stainless steel
TC	thermocouple
TDL	tunable diode laser spectrometer

This page is intentionally left blank.

ADVANCED CONCEPTS FOR DRY STORAGE CASK THERMAL-HYDRAULIC TESTING

This report fulfills milestone M3SF-19SN010203036 (Advanced concept for dry storage cask thermal-hydraulic testing with multiple fuel assemblies) in the Spent Fuel and Waste Science and Technology work package (SF-19SN01020303). This work was sponsored under the Department of Energy's (DOE) Office of Nuclear Energy (NE) Spent Fuel and Waste Disposition (SFWD) campaign.

1   INTRODUCTION

1.1   Objective

The purpose of this report is to review technical issues and previous studies relevant to the performance evaluation of dry storage systems during vacuum drying and long-term storage operations and to provide updates to vital experimental components under development that are required for conducting advanced studies.

There is a need to validate the extent of water removal in a multi-assembly dry storage system using an industrial vacuum drying procedure, as operational conditions leading to incomplete drying may have potential impacts on the fuel, cladding, and other components in the system. A waterproof, electrically heated spent fuel rod simulator has been developed to enable experimental simulation of the entire dewatering and drying process. In addition, specially-designed, unheated mock fuel rods are being developed to monitor internal rod pressures and study water removal from simulated failed fuel rods. Moisture monitoring instrumentation is also being considered to track water content within a dry storage system.

These fuel rod simulators and other advanced concepts are intended to populate a new thermal-hydraulic test apparatus with multiple fuel assemblies. This new dry cask simulator will bridge the prototypic complexity of the Department of Energy (DOE) and Electric Power Research Institute (EPRI) High Burnup Demo (Montgomery *et al.*, 2018) and the controlled environment of a lab-fielded apparatus as well as allow for the replication of commercial drying cycles. Furthermore, single assembly studies conducted previously cannot incorporate important inter-assembly heat-transfer physics, so plans for harvesting up to five full-length 5×5 truncated assemblies from commercial 17×17 pressurized water reactor (PWR) skeleton components are described.

This chapter will discuss important issues relevant to continuing experimental investigations on thermal-hydraulic assessments of dry cask systems. It will be followed by a discussion of past studies that have responded to some of these concerns experimentally. This will set the stage for an explanation of several test concepts in the next chapter.

1.2   Issues

1.2.1   Residual Water

Spent fuel assemblies are dried after interim storage in pools to ensure the removal of water in assembly cavities as a defense against issues related to pressurization and corrosion throughout the dry storage process. The evacuation of most water and oxidizing agents contained within the canister is recommended by NUREG-1536 (NRC, 2010). A pressure of 0.4 kPa (3 torr) is recommended to be held in the cask for at least 30 minutes post liquid water removal. A drying method similar to that developed at Pacific Northwest National Laboratory is suggested (Knoll & Gilbert, 1987), where less than 0.25 volume percent of oxidizing gases are left in the canister (1 mole in 7 m^3 at 150 kPa and 300 K).

An industry standard guide was established for the drying of spent nuclear fuel (SNF) after cooling in spent fuel pools (ASTM, 2016), although this includes no comprehensive treatment of safety concerns or

measures. The main purpose of the standard is to aid in the selection of a drying system and a means of ensuring that adequate dryness is obtained. Examples of typical commercial processes are documented in the standard, where there is adherence to the aforementioned 0.4 kPa level.

Water remaining in casks upon completion of vacuum drying can lead to corrosion of cladding and fuel, embrittlement, and breaching. There is also some risk of creating a flammable environment from free hydrogen and oxygen generated via the radiolysis of water. The remnant water may be chemically-absorbed (chemisorbed), physically-absorbed (physisorbed), frozen, or otherwise trapped in cavities, blocked vents, breached clads, damaged fuel, etc. Chemisorbed water is bound to contents by forces equivalent to a chemical bond, such as via the formation of hydroxides and hydrates on zirconium, or corrosion products on the fuel or cladding. Physisorbed water is bound to components by weaker forces (e.g. Van der Waals, capillary) as an adsorbate, and increased surface area provided through material defects enhances this effect.

The pressure applied during vacuum drying lies below the water vapor pressure. Given the unique heat retention and phase change properties of water, when significant heat is removed during volatilization, some quantity of liquid may actually freeze (ASTM, 2016). It is therefore important to understand under what marginal conditions ice may form during the procedure. As a preventative measure, it may be possible to use hot inert gases to create more uniform temperature profiles. Careful control of the vacuum pumps may also prevent ice formation by controlling the drying rate. This may be done by implementing pressure reduction in stages that involve bringing the temperature to equilibrium with inert gases like helium prior to commencement of the next stage. Further research and development on forced helium dehydration (FHD) has been recommended to address recently identified technological gaps (Hanson & Alsaed, 2019).

The removal of unbound water is largely dependent on the geometry and tortuosity of the components and the speed of the drying process. Cladding breaches are notable cases in that water can become trapped between fuel pellets and absorbed in cracks and voids. Water vapor may continue to be diffusively released after vacuuming. Depending on the thermal profile, condensation may occur on the cooler surfaces of the cask, which may lie at the lower extremes.

It is proposed that if vacuum is employed to remove water from a dry cask, measurements in the pressure response to intermittent pump operation may serve as a good indicator of residual, unbound water (ASTM, 2016). This approach would involve analysis of the time-dependent pressure rebound when the vacuum is turned off. The system may be adequately dry if the 0.4 kPa (3 torr) pressure can be sustained for at least 30 minutes. Spectroscopic techniques can also be employed to measure the mass of moisture removed.

1.2.2 Cladding Performance

Understanding cladding hoop stresses is critical for evaluating and predicting the mechanical integrity of the fuel rods. These hoop stresses have implications on corrosion, stress corrosion cracking, zirconium hydride reorientation, and creep. It is recommended to maintain pressure-induced hoop stresses in the cladding below 90 MPa to reduce the probability of hydride reorientation (NRC, 2003; Billone, Burtseva, & Han, 2013). During commercial operation, the internal rod pressure increases from the production of fission gases, the generation of gaseous decay products, and fuel pellet swelling, and overall these phenomena increase with burnup. If a clad is breached during operation, fission gases are released, and water can penetrate into the fuel through the gap. At the end of vacuum drying, canister pressures are reduced to as low as 0.4 kPa (3 torr), followed by pressurization to up to 800 kPa during storage. Pressure continues to rise from the initial backfill pressure via the release of gases from the fuel.

A technological gap exists in understanding the evolution of internal rod pressure during full-scale, heated experiments. Such measurements can provide valuable information on the state of stress in the fuel cladding as vacuum is applied during drying cycles.

1.2.3   Thermal Management

In the course of a typical vacuum drying cycle, the temperature of the fuel is liable to increase due to the reduction of thermal conductivity of the surrounding fluid. The peak cladding temperature (PCT) of the fuel should remain below 400 °C to minimize the potential for hydride reorientation in the cladding (NRC, 2003) which in turn results in alterations of mechanical cladding behavior. Furthermore, temperature gradients should be analyzed to identify areas where condensation of water vapor may occur in the cask, as condensation can lead to long-term, localized corrosion issues.

1.3   Previous Studies

1.3.1   Vacuum Drying Test Plan (CNWRA)

The Office of Nuclear Regulatory Research at the Nuclear Regulatory Commission (NRC) sponsored a report from the Center for Nuclear Waste Regulatory Analyses (CNWRA) in 2013 to develop a test plan for vacuum drying using the NUREG-1536 criterion (Miller *et al.*, 2013). A motivating concern was the verification of water removal after drying given the potential for ice formation, liquid blockage, and other physical means of water retention, although the report did not focus on chemisorbed water.

The first portion of the report identified industry equipment and procedures. The industry procedures had a common goal of avoiding ice formation and allowing for the system to reach equilibrium. First, bulk water is removed from the canister via the siphon port using a centrifugal pump. The canister is pressurized with dry helium and then depressurized with exhausted water and gas directed to the water trap. This is repeated until a minimum amount of water is observed in the siphon.

The drying process is performed in steps, where the vacuum is increased in a series of predetermined hold steps before reaching a final vacuum. At each hold step, the canister is isolated from the vacuum line and the pressure is monitored for a certain period of time, during which a pressure rise may occur if water evaporates. If the pressure rise exceeds a certain range during the time period, the step is repeated until a stable pressure is obtained. Three to seven hold points were observed among the manufacturers surveyed, with final pressures between 0.4 to 1.3 kPa (3 to 10 torr) held up to 30 minutes. Upon conclusion of drying, the canister is backfilled with helium to a desired pressure.

The report characterized components of the fuel assembly that would cause water to remain upon conclusion of drying including breached fuel rods. For PWRs, these include the top and bottom nozzles, spacer grids, and guide tube dashpots. For boiling water reactors (BWRs), these include the upper and lower tie plates, spacer grids, and water rods. The BWR water rods are plugged on the bottom but have holes along the lower axial length. With regards to the canister, the spacer disks and ends of the vacuum siphon tubes are likely to retain water.

The report described the experimental features needed or recommended for conducting a drying study. The recommendation was made to scale the diameter of the mock canister but not the length. The fuel assemblies must physically represent the components that may retain water listed previously. The assemblies must be heated to represent the decay heat for irradiated fuel, and the assemblies must be submersible in water at least to a depth that wets the water-retaining features. The experimental canister must therefore hold water, support a vacuum, and support final pressurization with helium. The experimental instrumentation must provide a detailed thermal characterization of the cladding through all of the drying operation steps as well as a detailed moisture balance. The previous studies discussed below are reviewed in the light of these CNWRA vacuum test plan recommendations.

1.3.2   High Burnup Demonstration

The DOE and EPRI High Burnup Confirmatory Data Project (or High Burnup "Demo") is an ongoing multi-lab demonstration of dry-storage aging effects on high burnup (HBU) fuel. It was meant to enhance

the technical basis for ensuring HBU SNF integrity and retrievability during continued storage and transportation.

Prior to cask closure, twenty-five fuel rods were removed from various assemblies and sent to Oak Ridge National Laboratory and Pacific Northwest National Laboratory. Nondestructive and destructive evaluations are underway to measure the mechanical performance of these HBU fuel rods (Scaglione, Montgomery, & Bevard, 2016; Montgomery *et al.*, 2018). End-of-life internal rod pressures have also been measured.

A TN-32B dry cask was loaded with HBU SNF consisting of 32 PWR assemblies from the North Anna nuclear power plant in Virginia. The cask was configured with thermocouple lances in the guide tubes of seven fuel assemblies, where each lance had a leak-tight penetration in the cask lid (each lance had 9 axially-spaced thermocouples, or TCs) (Csontos *et al.*, 2018; Hanson, 2018). Temperatures were measured on the cask exterior using an infrared thermometer. Ambient temperatures were also measured by thermocouples. Measurements were obtained during cask draining, drying, and storage. For the storage period, the measured PCT of 237 °C was much lower than the 318 °C result from the pre-test, design-basis-maximum simulation. While cask external temperatures aligned well with the models, the internal temperatures were overestimated by the models due to conservative geometric assumptions on the design of the cask internals.

Three gas samples were taken during the vacuum drying process. These samples were analyzed for residual moisture content and for the presence of fission gases. The samples indicated that no fission gases were present and that no liquid water remained in the cask (Bryan, Jarek, Flores, & Leonard, 2019).

As with most full-scale demonstrations, tight experimental control was limited. The temperatures measured during drying were lower than expected, but the final level of residual water may be higher than the recommended 0.25 volume percent (Knoll & Gilbert, 1987). Confirmatory measurement of the residual moisture is difficult and not possible unless the cask is opened again. While providing data for a prototypic system, additional data is needed to represent other dry storage systems and a broader parameter space.

1.3.3 Scaled Assemblies (University of Nevada, Reno)

A series of scaled assembly experiments were developed at the University of Nevada, Reno to benchmark simulations of SNF cladding temperatures during vacuum drying and transfer operations (Greiner, 2017). The project aimed to investigate the effect of a low-pressure environment on the PCT using both experimental and computational assessments. Both of the University of Nevada, Reno studies summarized below used heated assemblies that were truncated in length. No prototypic components were used, and many of the water-retaining features were not included.

An early experimental apparatus was employed from 2007 to 2012 consisting of a truncated 8×8 assembly of heater rods in a square enclosure (Chalasani, Araya, & Greiner, 2007). It aimed to validate computational fluid dynamics (CFD) simulations by measuring natural convection in the assembly gaps and thermal conductivity in the fuel rods and enclosure using strategically-placed thermocouples and a controlled heat rate. The apparatus was truncated axially to represent the spacing between two spacer grids in a BWR assembly and was configurable in both vertical and horizontal layouts to represent different stages of storage and transportation.

Another assembly was created in 2017 with a design truncated to 7×7 (Maharjan, 2018). This assembly was meant to simulate vacuum drying conditions and to benchmark CFD calculations. It also had the added capability of accommodating helium in the void space for rarefaction studies via flanges on the square enclosure, once again truncated in length to match the distance between two spacer grids. For the continuum regime of pressures (4 kPa to 200 kPa), the temperature difference between the central rod and average wall temperature was found to be nearly constant. However, in the slip regime (40 Pa to 2 kPa), the temperature difference increases with decreasing pressure because of gas rarefaction.

1.3.4 Single BWR Assembly, Full Length (University of South Carolina)

A NEUP integrated research project was conducted at the University of South Carolina on a full assembly-scale vacuum drying experiment for dry cask storage (Knight, 2019; Shalloo, Knight, Khan, Farouk, & Tulenko, 2017). The study aimed to demonstrate the application of vacuum drying using standard industry guidelines and provide data to validate drying models using a versatile experimental apparatus. At least 120 drying tests were conducted to analyze both "single" and "combined" effects. The single effect tests evaluated drying a set amount of water in a specific assembly or cask feature, such as a failed fuel rod, spacer disc, Boral sheet, BWR water rod, or PWR guide thimble dashpot. The combined tests focused on specific features following the flooding, dewatering, and blowdown of the apparatus and prior to the drying procedure.

Freezing was observed to occur in the spacer disk outside of the basket and rails and other specific tests involving spacers. These spacers are horizontal and are capable of holding water following blowdown. Nonetheless, the water was observed to melt in the holding period, leading to the dryness test failing and water being evacuated fully in a subsequent vacuum/hold step.

Tests with the failed fuel rod met test criteria for dryness (3 torr hold) and dehydration by helium (0.1% relative humidity) although between 7 to 12 cm^3 of water was still observed to be retained inside; this quantity was improved to 0.5-2 cm^3 with more carefully-controlled boundary conditions. Overall, retention was due largely to surface tension effects from tightly-packed ceria pellets, along with fractures that developed in the pellets themselves. Also, the hold-down springs in the failure test rods were mostly uncompressed and functioned as sites for liquid retention.

Twelve heater rods distributed throughout the fuel rod bundle were driven with power levels meant to simulate the overall dry cask decay heat. While remaining under the regulatory limit of 400 °C, the temperatures are observed to increase under vacuum and under helium gas recirculation. Tests that successfully brought the system to dry conditions corresponded to the highest heater rod temperatures, compared to those that had residual water. Test rod peak temperatures were obtained from thermal images and varied between 85 and 190 °C depending on the type of vacuum/helium test involved. Data is intended to inform predictive multi-phase, multi-physics models on vacuum drying.

Altogether, the heat flux profile and insulation played major roles in the overall behavior of results. Heat tape was added to the outside bottom of the chamber to reduce heat loss and prevent freezing in the siphon tube. It also allowed the cosine heat profile to flatten and more closely represent the typical profile of dry cask decay heat.

1.4 Desired Capabilities

Previous testing has provided a strong database and background from which to guide future test designs to meet remaining technical gaps (Hanson & Alsaed, 2019). The desired capabilities of these designs are summarized below.

1.4.1 Compatibility with Drying

The test apparatus should be capable of replicating commercial drying cycles. These include both vacuum and FHD drying cycles. Simulated fuel assemblies should be capable of heated operation during drying, which will likely require a submersible heater design. These assemblies should have prototypic, geometric features capable of trapping bulk water such as dashpots (PWR) and water rods (BWR). Furthermore, the apparatus should accommodate the testing of damaged fuel surrogates.

1.4.2 Prototypic Thermal-Hydraulics

The fuel assemblies should incorporate prototypic hardware and length scales to mimic the integral physics of dry storage systems. In lieu of a full-scale canister, a practical test approach recommended by the CNWRA report is to employ prototypic length and reduced diameter to emulate the length of relevant

industrial equipment – namely, the siphon tube and the fuel assemblies (Miller *et al.*, 2013). Additional considerations include properly incorporating the influence of gravity on heat transfer (i.e. natural convection) along the longitudinal axis when determining PCTs, as well as including the effects of axially-spread spacer disks as water entrapment points.

The test apparatus should be configurable to allow a variety of storage configurations to be studied. In addition, transportation configurations should be considered.

1.4.3 Monitoring of Cladding

The system should be capable of characterizing cladding behavior during drying and storage conditions. This characterization should include the measurement of cladding temperature and internal rod pressure. In order to achieve a realistic peak cladding temperature, the test fuel assembly needs to be populated with as many individually heated fuel rod simulators as is practical. The impact of cladding failures from pinhole to gross breaches should be considered.

2   DEVELOPMENT AND TESTING OF FUEL ROD SURROGATES

This chapter discusses updates to the development of new fuel rod simulators or surrogates and techniques for testing to address gaps in the current understanding of dry storage systems during drying and storage previously introduced in SAND2019-3587 R, "Component Concepts for Advanced Dry Storage Investigations" (Lindgren *et al.*, 2019). The updates in this report primarily focus on the progress made on submersible heaters. The ultimate goal is to employ these advanced heater rods in multiple assemblies in a versatile dry cask simulator for thermal-hydraulic experiments.

2.1 Test Objectives

Experiments were conducted to verify the performance of a waterproof electric heater rod in a pressurized stainless-steel (SS) vessel that can be partially filled with water. The heater is expected to improve upon the state of the art in current dry cask storage testing by accommodating complete submersion in water below the upper electrical connection points. This will allow for thermal hydraulic investigations of heater performance pertaining to water submersion effects, vacuum drying efficiency in residual free water removal, and the effects of backfilling with inert gas.

The main objectives of the test include the following:

1. Demonstrate that the rod can maintain full electrical performance while partially submerged in water, and that water can then be drained by gravity and a subsequent blowdown step.

2. Demonstrate that a sequenced vacuum drying procedure can be implemented where pressure measurements can confirm a steady-state holding pressure after the application of several hold points.

3. Demonstrate rod performance in a dry environment pressurized with inert gas or air while obtaining temperature and pressure measurements over time.

Performance verification in these single heater experiments may allow more advanced vacuum drying tests to proceed that can employ several of these rods in assemblies, which in turn can provide data scalable to industrial dry cask storage and transportation applications.

2.2 Submersible Heater

A new heater rod concept was developed that will enable the assessment of thermal phenomena in a wet environment. These rods are partially-submersible versions of those in past designs, with immersion planned for a significant extent of the axial length. They are comprised of magnesium oxide (MgO) compacted around a spirally-wound Nichrome wire with cold pins on either end, as shown in Figure 2.1. The coil is wound in a helix that is approximately the radius of the cold pin. Magnesium oxide ceramic was selected as a surrogate fuel material due to similar thermal mass (ρC_p) behavior with increasing temperature relative to SNF (Lindgren & Durbin, 2007).

Each heater features a top fitting with a hermetic ceramic-to-metal bond (Figure 2.2) that allows connection to the power source, while electrically isolating the cladding and protecting the MgO from moisture. The top fitting is welded to the pin at the upper extreme of the threaded pin cover, along with brazing between the sheath at the clad/seal interface. The bottom fitting has similar geometry to a bottom fuel plug, with an internal blind hole containing high-temperature electrical grease to receive the neutral cold pin. This bottom plug is circumferentially welded to the cladding, effectively bonding the cladding to the electrical neutral (see Figure 2.3). The cladding is therefore electrically isolated from the hot connection via the top hermetic seal. In lieu of an electrically connected bottom fitting, the neutral is drawn from a wire attached near the upper portion of the cladding.

Electrical power ("hot" connection)

Threaded pin cover

Ceramic-to-metal hermetic seal

Sheath

Neutral wire

K-type thermocouple

← To DAQ

Line cold pin

Nichrome coil

Nichrome shim

Cladding

MgO

Neutral cold pin

Conductive paste

End cap

☀ = Spot weld
◉ = Braze
◉ = Circumferential weld
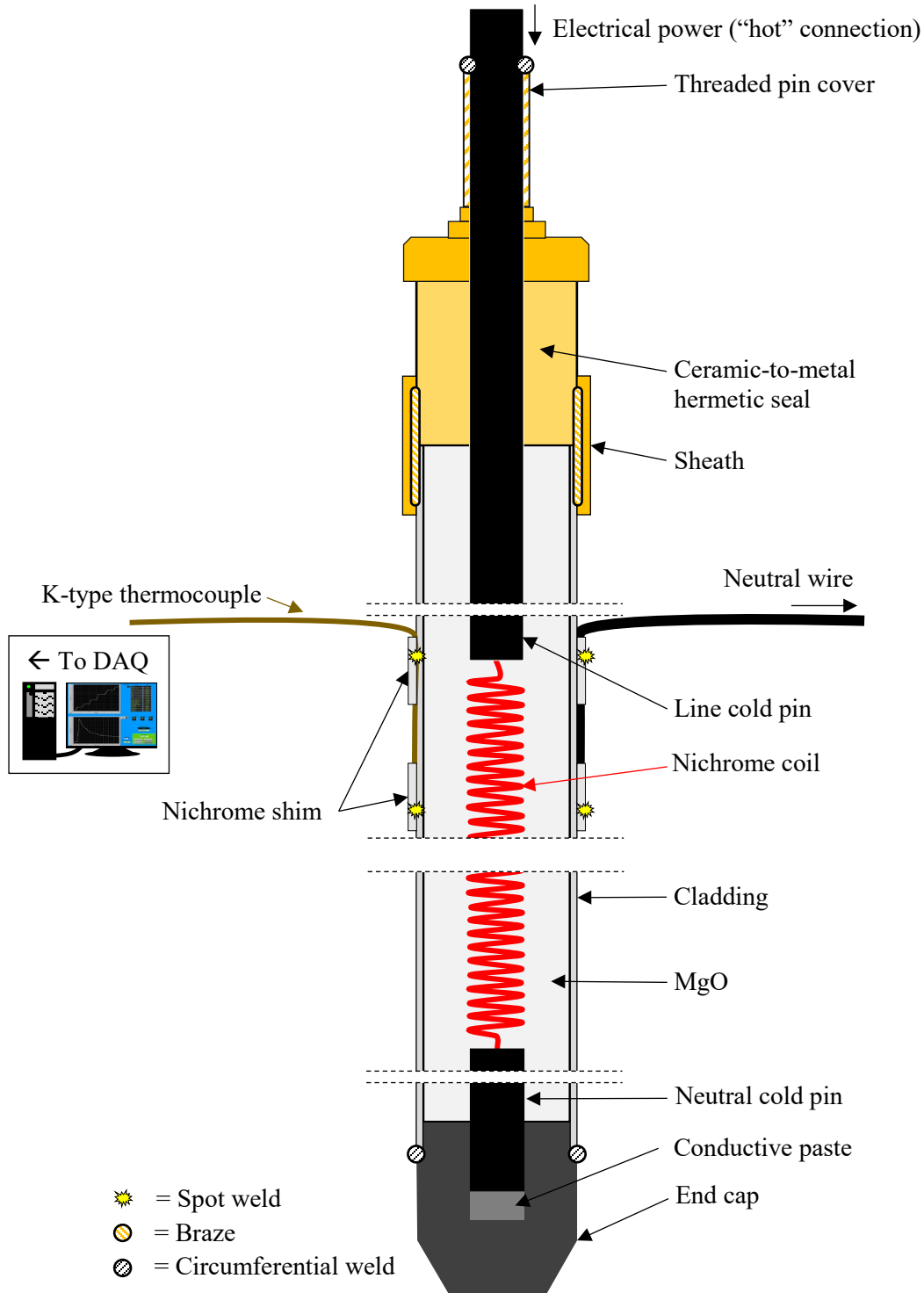
Figure 2.1   Heater rod diagram (see schematic view in A.1).

Figure 2.2   View of threaded connection, hermetic seal, and heater sheath.

Figure 2.3   View of the welded end plug on the 1000 W heater.

2.3 Pressure Vessel

The pressure vessel is shown in Figure 2.4 and consists of 1 in. nominal pipe size 304 SS Schedule 40 pipes joined by Class 150 304 SS fittings and valves. The Class 150 components limit the maximum allowable working pressure (MAWP) of 1,030 kPa (150 psi). The main test section consists of two pipe nipples, a 914 mm (36 in.) and a 152 mm (6 in.), two pipe crosses, and a pipe tee. The penetrations in the vessel are Conax fittings that allow feedthroughs for the electrical line and neutral as well as thermocouples that are connected to the data acquisition system (DAQ). The Teflon packings had a temperature limitation of 232 °C and required the use of SS pipe standoffs to increase the distance between the electrical feedthroughs and the heater. A 165 mm (6.50 in.) long SS pipe separates the neutral fittings and the middle cross. Similarly, a 305 mm (12.0 in.) long SS pipe separates the electrical power fittings and the top of the upper cross. The pipe nipple in the upper cross connecting the tee with the pressure relief valve (PRV) is 140 mm (5.50 in.) in length due to the valve temperature rating of 200 °C.

The ball valve leading to the top cross is meant to isolate the pressure vessel from the pressure and vacuum lines and is normally open except during water fill operations, when it is closed to protect those lines from accidental overflow. The ball valve at the bottom tee is used to allow for the filling and draining of water, and the ball valve at the middle cross is an overflow valve meant to keep the water level below both the neutral weld (in the 152 mm (6.00 in.) pipe between the middle and top crosses) and the electrically hot connection in the top cross. More details of the pressure vessel and pressure system are shown in Section A.2 and Appendix B.

The pressure vessel was protected from pressures at or above the MAWP via one PRV directly in line with the SS pipe, and another on the pressure fill line for redundancy. Either valve has an exhaust feature to manually vent the system. It is anticipated that boiling water could provide a source of overpressure if the gas cylinder is isolated from the vessel. The pressure system is described in detail in Appendix B,

although some components, such as the gas drying unit, pressure switch, and actuated solenoid valve, could not be implemented in time for this test series.

Figure 2.4   Pressure vessel and mount.

2.4 Instrumentation

2.4.1 Thermocouples

A diagram of thermocouple locations is shown in Figure 2.5. The cold pins, approximately 150 mm (6.0 in.) in length, on either end of the heater impart limitations on the locations that are chosen. A spacing of 203 mm (8.00 in.) beginning at the tip of the end cap was chosen to provide eight pairs of thermocouples located on the outside of the heater and the outside of the 914 mm (36 in.) pipe (as opposed to pipe connectors) for consistency and extensibility of data. However, two TCs were also placed on the 152 mm (6.00 in.) upper pipe to monitor temperature in the unheated region.
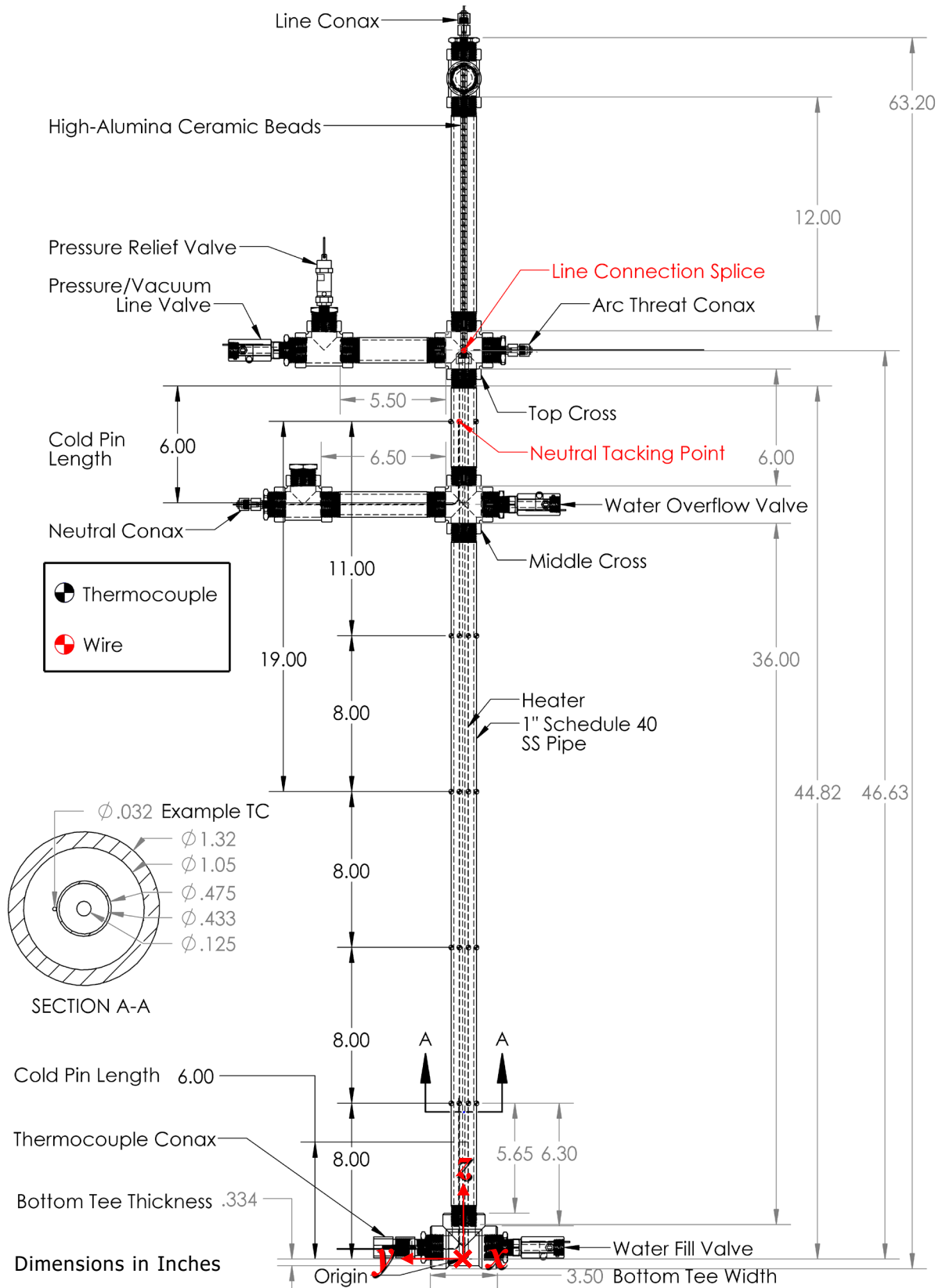
Figure 2.5   Schematic of thermocouple locations with dimensions in inches.

A list of thermocouples is shown in Table 2.1 with axial coordinates and orientation with respect to the testing facility. The origin is defined as the center of the tip of the welded end plug on the heater rod. A right-hand coordinate system is employed based on the z-dimension increasing from the welded plug to the hot connection, where the x-dimension increases towards the mounting board and the y-dimension moves northward. It is indicated whether the TC is attached on the heater rod inside of the pressure vessel (Int) or on/external to the outer surface of the pressure vessel (Ext).

The limitation of eight internal TCs was determined by the number of penetrations in the sealing gland. All internal TCs were routed from the feedthrough on the bottom tee to the DAQ. The ambient TC was located on the DAQ approximately 1.8 m (6.0 ft.) away from the pressure vessel.

Table 2.1   List of thermocouples (type K).

Channel	x-position (in.)	y-position (in.)	z-position (in.)	Direction	Int/Ext	DAQ Label
1	0	0.24	8.0	North	Internal	08.00" North Int
2	0	-0.24	8.0	South	Int	08.00" South Int
3	0	0.24	16.0	North	Int	16.00" North Int
4	0	-0.24	16.0	South	Int	16.00" South Int
5	0	0.24	24.0	North	Int	24.00" North Int
6	0	-0.24	24.0	South	Int	24.00" South Int
7	0	0.24	32.0	North	Int	32.00" North Int
8	0	-0.24	32.0	South	Int	32.00" South Int
9	0	0.66	8.0	North	External	08.00" North Ext
10	0	-0.66	8.0	South	Ext	08.00" South Ext
11	0	0.66	16.0	North	Ext	16.00" North Ext
12	0	-0.66	16.0	South	Ext	16.00" South Ext
13	0	0.66	24.0	North	Ext	24.00" North Ext
14	0	-0.66	24.0	South	Ext	24.00" South Ext
15	0	0.66	32.0	North	Ext	32.00" North Ext
16	0	-0.66	32.0	South	Ext	32.00" South Ext
17	-	-	-	North	Ext	Ambient
18	0	0.66	43.0	North	Ext	Top 6" Pipe North
19	0	-0.66	43.0	South	Ext	Top 6" Pipe South
20	3.25	0	37.5	West	Ext	Face of Board

2.4.2 Pressure Transducers

A Setra AccuSense (model ASM1150PA1M2CO3A01) with a range of 0 to 1,034 kPa (0 to 150 psia) and accuracy of ±0.05% of full scale was used as an absolute pressure transducer (PT). This transducer uses a resonant variable capacitance sensor, which is calibrated via a curve-fitting algorithm to optimize the sensor's linearity. The maximum recoverable pressure that can be applied to this instrument without changing its performance is 8,274 kPa (1,200 psi). An Omega high-accuracy, oil-filled pressure transducer (model PXM409-001BV10V) with a range of 0 to 100 kPa (0 to 14.5 psia) and accuracy of ±0.08% of the compensated range was used as an absolute vacuum-level pressure transducer.

2.5 Mount

The pressure vessel is mounted vertically on one side of a wooden board held upright by a Unistrut frame, as shown in Figure 2.4. The pressure, vacuum, and water lines are mounted on the other side of the wooden board for operational safety, as the pressure and filling material could be adjusted while the heater is energized and the vessel is hot. Conductive heat transfer is limited by the use of thermally-insulating standoffs at the middle cross (fiberglass, Figure 2.6) and bottom tee (Duraboard). No external insulation was used for the pipes; therefore, ambient temperature fluctuations at the test facility due to open doors, fans, and weather had the potential to affect vessel temperatures.

Figure 2.6   Middle cross of pressure vessel tied to fiberglass bracket with Nichrome wire.

2.6 Power Control and Measurement

The electrical voltage and current delivered to the heater rod were controlled to maintain a constant power level by a digital silicon-controlled rectifier (SCR). The device software provided a digital power setpoint to the SCR that was controlled based on internal feedback. However, to have a calibrated reference, manual measurements of the current and voltage were taken with Fluke meters, which were then used to manually adjust the SCR setpoint to the desired power. Table 2.2 lists the instruments used for power control and measurement, and Figure 2.7 shows the power control setup. For the 1000 W heater rod, 10-amp fuses were installed in the circuit in the event that the heater rod was shorted during the tests. The full-scale settings for SCR control were defined as 1000 W, 120 V, and 8.333 A. The SCR and pressure vessel shared the same ground as the power source.

Table 2.2   List of power control equipment.

Description	Manufacturer	Model
Digital SCR AC Power Controller	Control Concepts	uF1HXLGI-130-P1RSZ
DC Power Supply, 30 V, 3A	BK Precision	1735A
Voltmeter	Fluke	789 ProcessMeter
Clamp Ammeter	Fluke	381 Remote Display TRMS
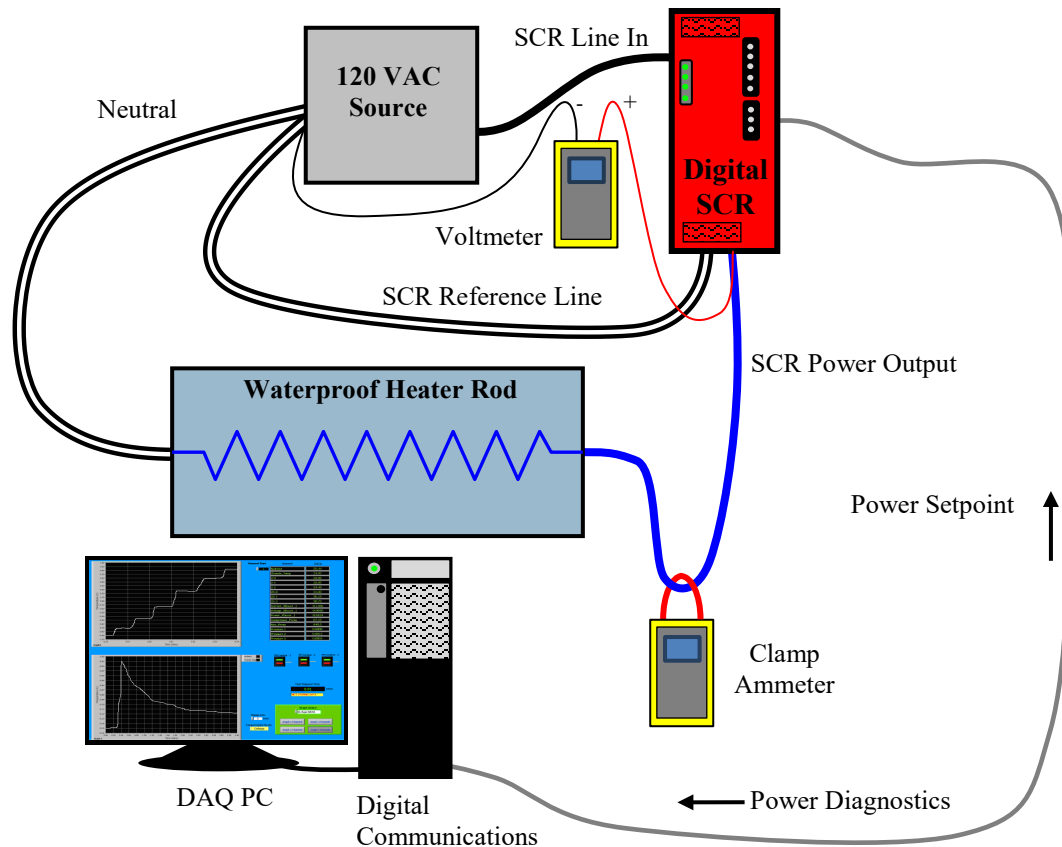
Figure 2.7   Power control setup.

2.7 Fuel Rod Surrogate Testing

A series of tests were planned to verify heater rod performance for the wetted and pressurized conditions that would be expected in a full-scale test with multiple rods. The rod must maintain an uninterrupted electrical connection during scaled demonstrations of various stages of industrial drying and storage operations, including inundation with water, blowdown, vacuum drying, and final backfill.

2.7.1 Water Filling and Heating Test

The goal of the water filling and heating test was to verify that the heater can be partially submerged in deionized water while it is energized. The neutral, while connected above the water line, relies on wire insulation and a feedthrough to run through the water and out of the pressure vessel. In this test series, water was pumped into the pressure vessel without flooding the hot connection. The heater was then powered while surrounded by water for most of its heated length. Temperature measurements were monitored by the operator to ensure that the maximum thermocouple reading on the exterior of the rod does not reach boiling conditions in Albuquerque, NM (94 °C). After an extended time period, the water was drained from the system first via gravity and then through pressurized blowdowns. The efficiency of the blowdowns was measured by the amount of additional water discharged after the initial drainage.

2.7.2 Vacuum Drying Test

This test applied sequential vacuum hold points to verify heater performance in evacuated conditions and investigate pressure rebound due to residual water evaporation remaining after a blowdown. Therefore, the vacuum drying test was conducted after the water filling test in order to have some quantity of free water in the vessel. Pressure measurements were monitored by the operator for three 30-minute holding

periods. The hold procedure was halted if the operator observed a steady-state pressure. Temperature measurements were monitored to ensure that the maximum thermocouple reading on the rod did not exceed the Conax insulator limitations.

2.7.3 Backfilling Test

This test verified that the heater can maintain electrical performance in an environment pressurized with air or inert gas. Pressure and temperature measurements were obtained over time, and temperature was monitored to ensure that the maximum thermocouple reading on the exterior of the rod did not exceed the Conax insulator limitations. Because actuated needle valves were not available to maintain the pressure at a certain level, the pressure level was maintained through manual operation of ball valves and the gas cylinder regulator. (More details about the pressure system of the enclosing vessel can be found in Appendix B.)

2.8 Test Matrix

The test matrix is shown in Table 2.3. The individual tests for the waterproof heater rods were parametrized by the fluid filling the pressure vessel (air, helium, deionized water, or vacuum), the pressure level(s), the power applied to the heater, and the type of current from the power supply.

Table 2.3   Test matrix for the waterproof heater rod.

Test Series	Test	Internal Fluid	Pressure (kPa)	Power (W)
Water Filling and Heating	1	Deionized Water	84.1 (Atmospheric)	40
	2	Deionized Water	84.1 (Atmospheric)	58
	3	Deionized Water	84.1 (Atmospheric)	75
Gravity Drainage and Blowdown	4	Deionized Water	345	0
Vacuum Drying	5	Deionized Water	0.2 (Max Vacuum)	58
Backfilling	6	Helium	600	40
	7	Helium	800	58
	8	Air	800	58

This page is intentionally left blank.

3   WATERPROOF HEATER ROD TEST RESULTS

3.1 Water Filling Test

The verification of the functionality of the waterproof heater rod while submerged in deionized water was carried out through the monitoring of power output to the heater rod over the course of a 6-hour energized test run. The power was ramped up under close monitoring by an operator to ensure that the temperatures throughout the test apparatus did not exceed the boiling point of water in Albuquerque, NM (94 °C), in order to avoid shorting of the heater rod. As a proof of concept, the test was considered successful if the heater rod did not short throughout the duration of the test.

3.1.1 Water Filling and Heating

The power output from the SCR was found to differ from that calculated from the voltage and current measurements from the Fluke instruments. These instruments are calibrated, direct line measurements and considered more accurate than the SCR. Therefore, an iterative procedure was carried out under dry, atmospheric conditions (before water was pumped into the apparatus) to calibrate the SCR fieldbus setpoint such that the Fluke measurements would indicate the actual desired power. This involved manually adjusting the fieldbus setpoint from an initial value until there was reasonable agreement with the power directly measured on the line.

The temperature limitation for these tests was set by the Teflon insulators for the electrical Conax fittings, which have an upper operational temperature bound of 232 °C. It was found that at 58 W, the highest temperature present towards the top of the heater rod was 240 °C. As mentioned previously in Section 2.3, standoffs were employed to provide separation between the electrical feedthroughs and the heater, resulting in much cooler temperatures at the fitting locations. This allowed for a reasonable safety margin for heater operation at or just above the 232 °C threshold.

Under atmospheric and de-energized conditions, water was successfully pumped into the pressure vessel without flooding the hot connection, demonstrating a key operational principle of the heater and vessel design. (A water mass balance will be described in more detail in Section 3.1.2.) Once filled, setpoints of 40 W and 58 W were chosen to gradually ramp up power based on the iterative power test. When it was observed that the temperatures would not exceed 75 °C at 58 W, a higher setpoint of 75 W was chosen in an attempt to raise the maximum test apparatus temperature as close as possible to 94 °C to stress the system.

Figure 3.1 shows the temperatures reached over the course of the 6-hour test run as well as the power output measured from both the SCR and the Fluke instruments. The two figures use the same time scale, so the ramps in power correspond to the temperature. The slow rise in temperature observed near the end of Test 1 is due to the increase in ambient temperature as the test facility did not have climate controls in place. The fluctuations in temperature seen after the ramp in power to 75 W were due to the operation of a swamp cooler in the test facility that caused the test environment to cool. While the overall extent of this cooling was not anticipated, it was shown to provide an additional method of temperature control for future experiments, especially those that could bring temperatures closer to 94 °C. The cooling effect was mitigated shortly after five hours when the direction of the cooler was turned away from the pressure vessel and mount.

Figure 3.1 shows that continuous heater operation is present over the course of the water filling and heating tests because no short is detected. Therefore, it can be concluded that the heater rod is operable under partially submersible conditions.
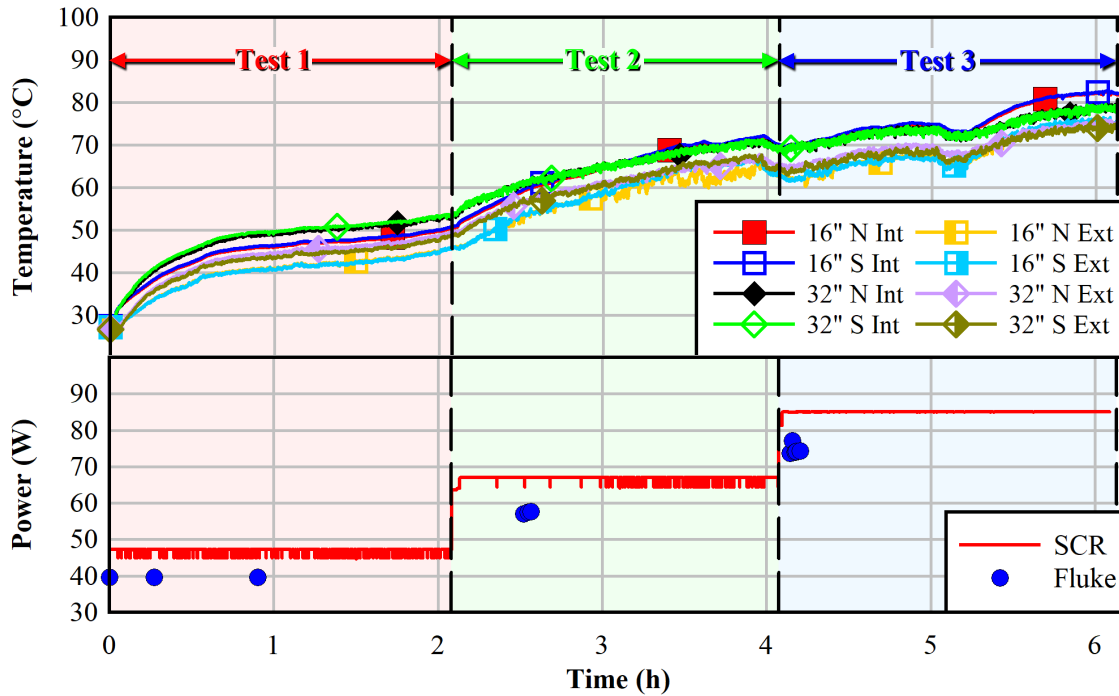
Figure 3.1 **Temperatures of the hottest thermocouples (upper) and the SCR and Fluke instrument power outputs (lower) as a function of time for the water filling and heating test.**

3.1.2 Water Draining

The water drainage procedures (Test 4) incorporated both gravity drainage and a pressurized blowdown in order to remove bulk water prior to vacuum drying. For this test, water removal from the pressure system was accomplished immediately after the water filling and heating test. The heater rod was de-energized after the conclusion of Test 3 and the start of Test 4. The water was then removed during the cooldown.

A container, shown in the bottom right of Figure 2.4, was used to collect water and quantify the mass balance in order to determine the effectiveness of either drainage mechanism. The container was weighed on a 0.5 g (0.001 lb) precision scale after each procedure and tared. Any differences would demonstrate the effectiveness of implementing a blowdown on the heater rod. An aluminum foil cover was placed over the container to prevent losses due to splashing, although some losses were introduced via unmeasurable condensation on the foil.

The water drainage procedures were conducted as follows. First, water from a tank was pumped into the water line and pressure vessel until excess water flowed into the container. The weight of the excess water in the container was measured to be 0.231 kg. The total amount of water pumped through the system was measured by weighing the water tank before and after the pumping step and taking the difference – this value was 0.928 kg. The amount of water in the water line and the pressure vessel was thus the difference between the total amount of water pumped through and the excess water in the container – this was 0.697 kg.

For the gravity drainage step, the drain valve at the bottom tee was opened. The water that was emptied into the container solely from this step was weighed – this value was 0.289 kg. The blowdown was then conducted with compressed air, and the system was pressurized until a pressure of approximately 345 kPa (50.0 psi) was read on the DAQ. At this point, this drain valve was opened until the pressure read approximately 124 kPa (18.0 psi) before re-pressurizing. This was done once at 276 kPa (40.0 psi) and four times in succession at 345 kPa (50.0 psi) (see Figure 3.2). After the blowdown procedure, the water

exiting the pressure vessel solely from the blowdown procedure was measured – this value was 0.022 kg. The total amount of water exiting the pressure vessel from the gravity drainage and blowdown steps was thus 0.311 kg.
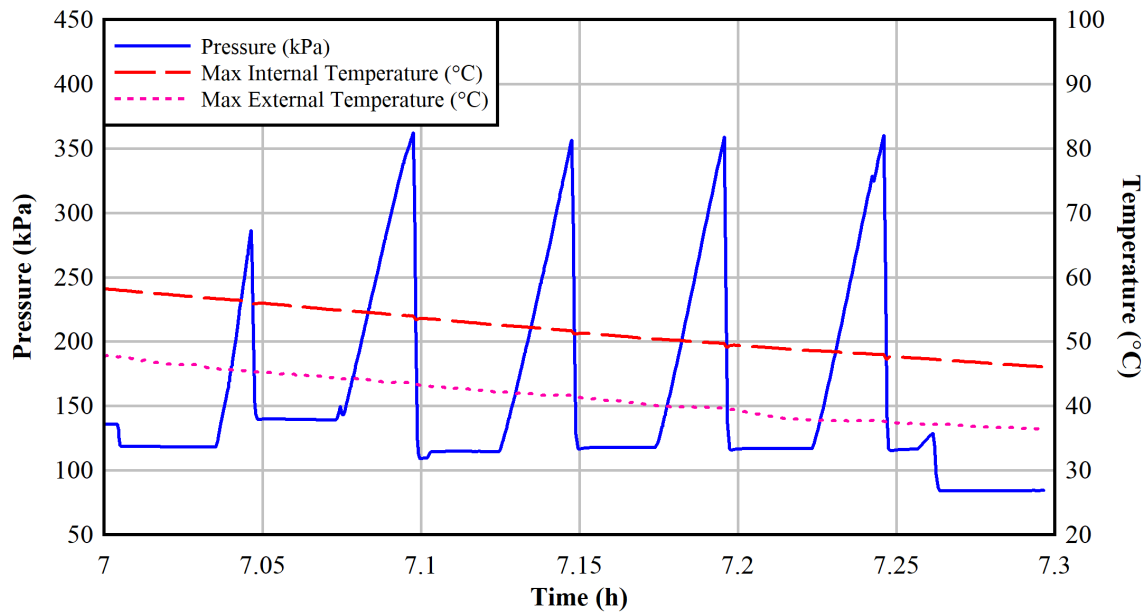
Figure 3.2   Pressures applied during the blowdown procedure immediately following the water heating test.

Measurements of water throughout the drainage procedure are shown in Table 3.1. A difference of 0.386 kg of water was measured between the initial water mass in the system and the amount recovered. The rotameter in the water pump line retains approximately 0.17 kg of water, which accounts for 56% of this mass. The remaining 0.218 kg of water was likely lost through evaporation during heated testing (Tests 1 through 3).

Table 3.1   Water draining weight measurements.

Water Draining Step	Item	Weight (kg)
Water Fill	Total water pumped	0.928
	Overflow	0.231
	Total initial water in system	0.697
Water Recovery	Water recovered via gravity drainage	0.289
	Water recovered via blowdown after four steps	0.022
	Total water recovered	0.311

3.2 Vacuum Drying Test

3.2.1 Preliminary Measurements

A Pentair A31 vacuum-rated needle valve was installed on the vacuum line in order to emulate the industrial procedure of implementing increasingly lower levels of vacuum with each hold point. However, preliminary testing with the Leybold-Heraeus Trivac D4A pump indicated that fine manual control of the vacuum level could not be realistically achieved with that valve. Therefore, the valve was kept fully open for the duration of testing and the vacuum level was at full capacity.

A vacuum leak test was carried out at room temperature prior to the drying test when no water was yet introduced into the system. The result of the leak test is shown in Figure 3.3. The leak test demonstrated that the pressure vessel had a leak rate of 44 torr per hour. This leak rate was assumed to be independent of temperature and used to correct the vacuum measurements in the drying data in the next section.

The authors recognize that the leak rate of the pressure vessel and system implemented for this test series requires improvement in order to accurately measure residual free water removal during drying tests. However, a preliminary series of drying tests were conducted with the as-built system to demonstrate the proof of concept and test the availability of the selected instrumentation.
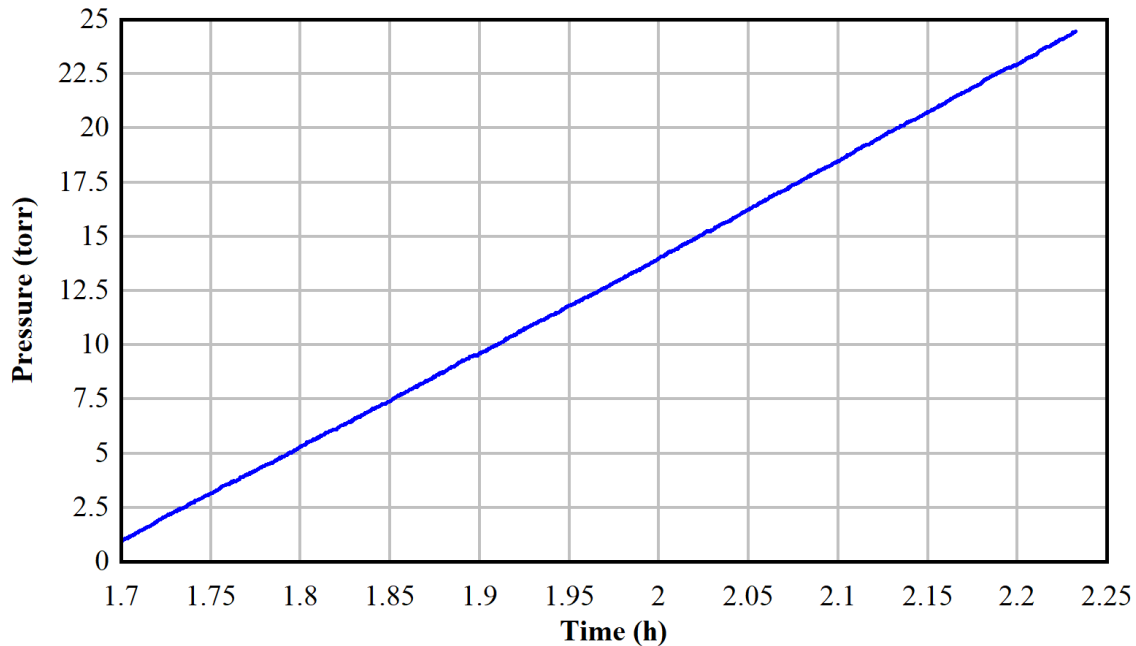
Figure 3.3   Pressure leak test after evacuating the vessel and isolating the vacuum line at ambient temperature.

3.2.2 Drying Results

The effectiveness of vacuum drying on removing residual free water from the waterproof heater rod system was tested by applying sequential vacuum holds for 30-minute periods in Test 5. Residual water being released from interior surfaces would manifest as a pressure increase due to the introduction of water vapor into the system.

The vacuum pump was operated at maximum capacity for each vacuum hold as a proof of concept to show pressure fluctuations due to residual water being removed from adsorption sites in the vessel. To simulate the presence of decay heat from spent fuel during vacuum drying, a maximum power of 58 W was supplied to the heater rod for the duration of the test. A voltage of 24.98 V and current of 2.3 A was measured by the Fluke meters to confirm that 58 W of power was actually imparted to the load. However, power was applied directly after the blowdown, so the system was in a cool state before the procedure commenced.

The Omega vacuum transducer provided output scaled to the total differential pressure referenced to ambient pressure, as opposed to an absolute pressure. To convert to absolute pressure, the average ambient reading from the transducer, 0.400 kPa (0.058 psi), was used along with the pressure reading for atmospheric pressure at the test site, 84.116 kPa (12.200 psi).

The results of the vacuum drying test over three successive vacuum pump/hold steps are plotted in Figure 3.4. The behavior of the data corresponds to the following events: 1) active vacuum pumping, 2) isolation of the vacuum pump from the test section with an immediate increase of ~8 torr in system pressure, and 3) pressure increase during the hold before the next evacuation. The leakage-corrected pressure shown in Figure 3.4 assumes extensibility of the leak rate observed in the dry test to a wetted environment at higher temperature. The authors note that the leak-corrected rate of rise derived during the three vacuum cycles is the same order of magnitude as the actual leak rate. Therefore, the accuracy of these results should be viewed as limited.
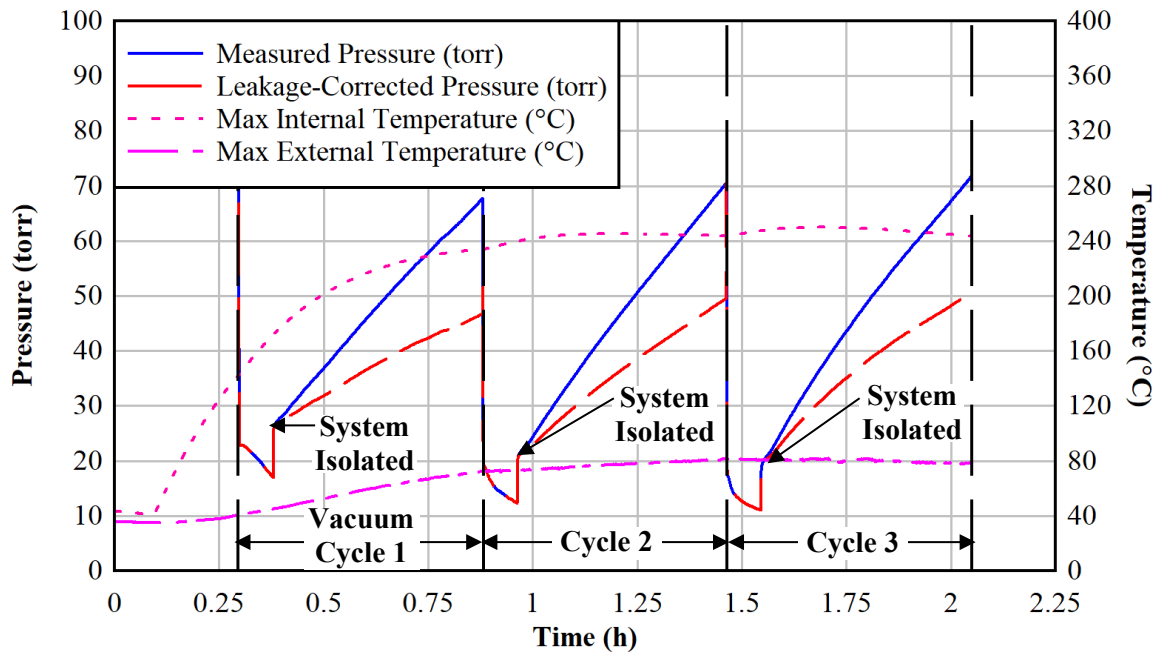
Figure 3.4 **Pressure versus time for the vacuum drying test with both measured data and a dry leakage rate correction.**

Table 3.2 shows the unadjusted rate of pressure rise for the period just after the sharp pressure increase during system isolation to the end of the hold. The pressure rises observed in the three holds were greater than or equal to twice the leak rate. However, pressure increases due to system heating were calculated to be < 3 torr, so the rise in pressure from water vapor cannot be excluded either. The internal temperatures in this test reach 250 °C, which is on par with the temperature generated under atmospheric conditions with the optimal 58 W power level.

Table 3.2   Pressure changes during the vacuum holds.

Vacuum Cycle	Event	Time (h)	Pressure (torr)	During System Isolation		
				ΔP (torr)	Δt (h)	Rise rate (torr/h)
1	Active pumping	0.290	630.9			
	System isolated	0.380	17.0			
	Hold	0.381	26.0	41.8	0.499	82.8
	End hold	0.880	67.8			
2	Active pumping	0.883	19.8			
	System isolated	0.963	12.3			
	Hold	0.964	20.2	50.4	0.499	100.8
	End hold	1.463	70.6			
3	Active pumping	1.465	18.4			
	System isolated	1.546	11.0			
	Hold	1.548	19.0	52.7	0.5	104.4
	End hold	2.048	71.7			

Within the pressure vessel, several sites exist for the retention of water in the form of thermocouples, the electrical wires, centering washers (with flow holes), pipe threading, and physical defects in the materials. Nonetheless, the geometry of the system is simplified compared to a prototypic spent fuel assembly, which contains numerous water retention sites. A simplified system would result in a greater likelihood of complete residual water removal during the drainage and blowdown steps. However, refinements to the test apparatus and procedures in this single rod system are needed to make better assessments. Fine vacuum control as opposed to 100% full vacuum is also needed for the procedure to be more prototypic.

3.3 Backfilling Test

The verification of waterproof heater rod performance under pressurized conditions in both helium and air was carried out via backfilling tests, where the pressure system was filled up to 800 kPa (116 psi). Figure 3.5 shows the power supplied to the heater rod with helium at 600 kPa (87.0 psi), while Figure 3.6 shows the power with 800 kPa (116 psi) helium. Figure 3.7 shows the results of the backfilling test using 800 kPa (116 psi) air. Once again, the SCR power output was calibrated so that the power calculated from the Fluke instruments was 58 W. The consistency in the power supplied to the heater rod over the course of both backfilling tests demonstrates that the waterproof heater rod is capable of sustained operation under pressurized conditions. The heater functioned as expected without incident during all pressurized testing.
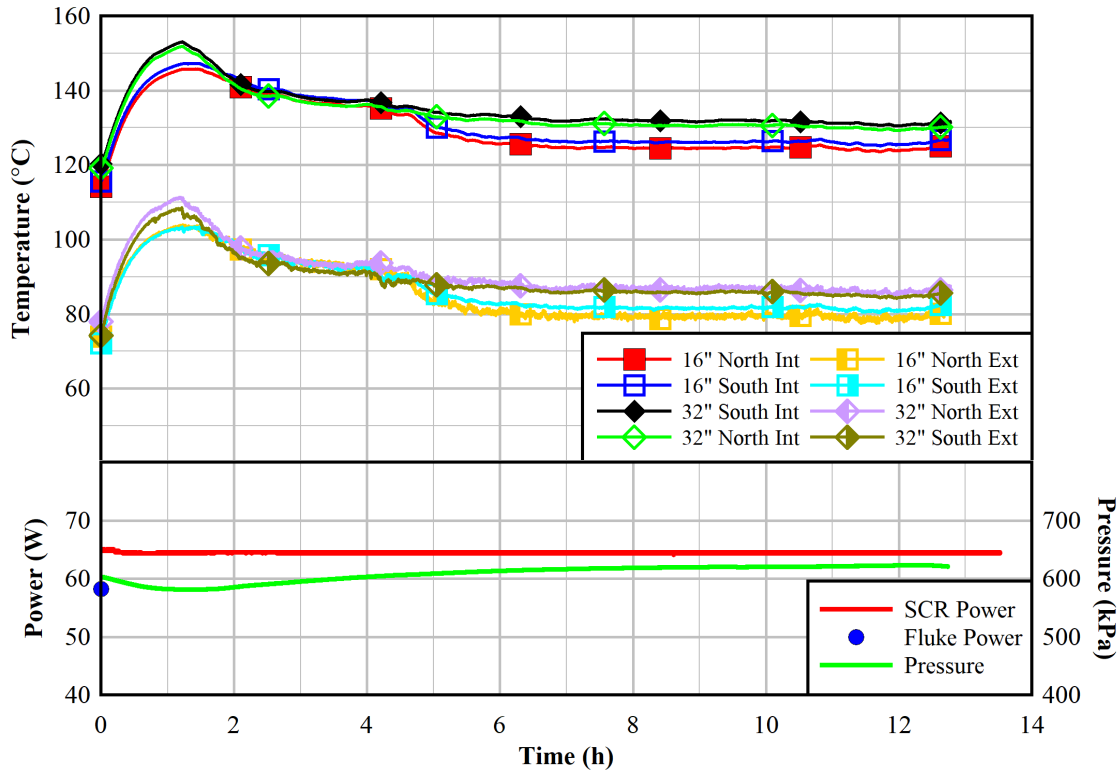
Figure 3.5 Temperatures (upper) and power input and pressure (lower) versus time for the 600 kPa helium backfill test.
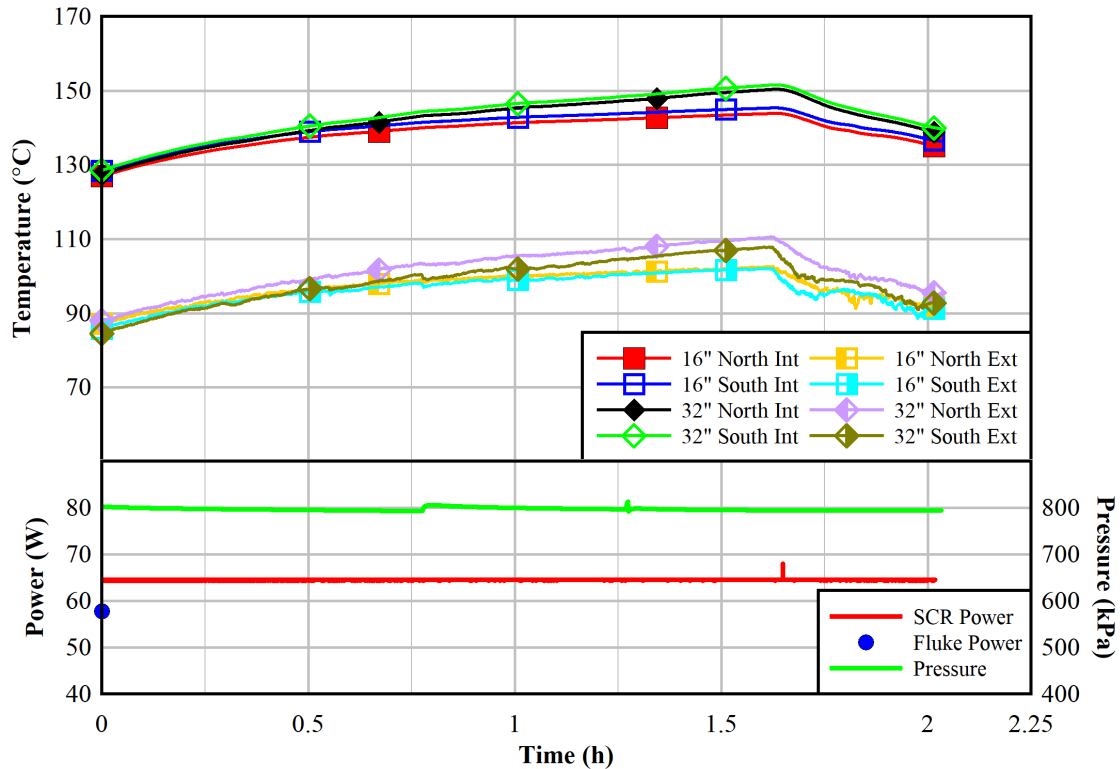

Figure 3.6 Temperatures (upper) and power input and pressure (lower) versus time for the 800 kPa helium backfill test.
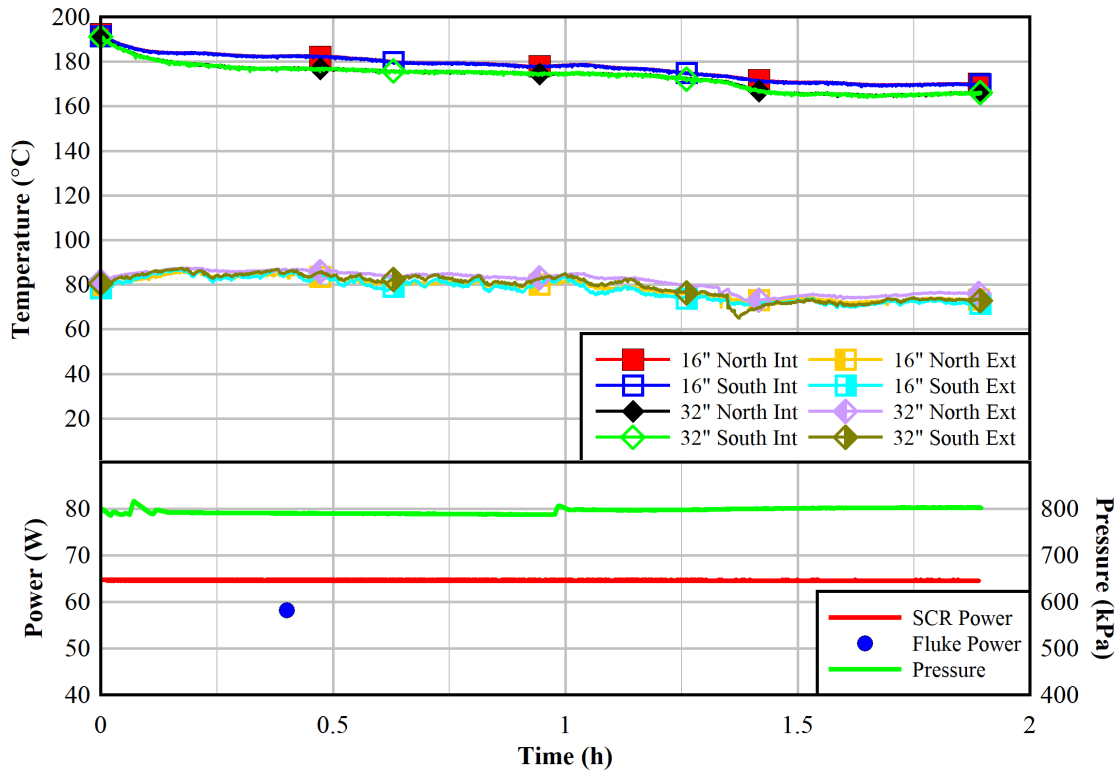
Figure 3.7   **Temperatures (upper) and power input and pressure (lower) versus time for the 800 kPa air backfill test.**

4 FUTURE ADVANCED TESTING CONCEPTS

Additional concepts are under development that can collect more information from an advanced dry cask simulator with multiple fuel assemblies. This chapter describes these concepts that can be tested to determine their potential applicability in advanced studies.

4.1 Separate Effects Tests

The effects of cladding oxidation and crud on water retention in dry storage systems can be explored via separate effects tests (SETs). This would involve smaller-scale tests that would measure chemisorbed and physisorbed water content on samples of cladding with existing oxidation and crud. Initial guidance regarding this data retrieval may be taken from the Sister Rod nondestructive examination efforts (Montgomery *et al.*, 2018). With this information, a coordinated focus from SETs and the advanced simulator work would be centered on incorporating these water retention properties either into cladding analogues or cladding with recreated oxidation and crud layers.

4.2 Internal Pressure Monitoring Rod

An unheated fuel rod can be inserted into the fuel assembly to measure the internal rod pressure. While end-of-life internal rod pressures are well characterized through testing and modeling, the effect of transient thermal cycles, such as those encountered during the drying of a spent fuel canister, are not well understood. Measuring the internal pressure directly while simultaneously simulating a near-prototypic drying cycle with detailed axial and transversal temperature data would provide valuable insight into the additional stresses imposed on the cladding.

The pressure monitoring rods can be constructed in a similar fashion to a previous study (Durbin, Lindgren, & Humphries, 2016). The fuel rods are loaded with surrogate pellets and prototypically-shaped end plugs are welded to the cladding. A small diameter, thick-walled tube connects the fuel rod to an external pressure source and transducer allowing the transient measurement of internal rod pressure. Figure 4.1 shows a schematic of a pressure-monitoring rod, where the top fitting is circumferentially welded to the pressure tube.

4.3 Breached Cladding Rod

Defects can be introduced to the cladding of the unheated rods described in Section 4.2 for studies on breached fuel rods. As shown in Figure 4.2, cladding breaches can be introduced at a specified axial location with a set geometry. A breach may include a pinhole leak, hairline crack, or gross rupture (larger than 1 mm). A breach can be machined into the cladding with well-defined geometry. Water would be metered into the breached rod through the small diameter, thick-walled tubing. The same tubing would then be used to monitor the pressure inside the rod during a heated drying test. The differential pressure between the breached rod and the pressure vessel will be used in the evaluation of the breached rod drying.

Magnesium oxide (MgO) is a possible surrogate fuel material due to similar thermal mass (ρC_p) behavior with increasing temperature relative to SNF (Lindgren & Durbin, 2007). The choice of MgO will allow the heater material and pellets to be representative of the thermal mass of a fuel rod. However, the MgO ceramic is slightly porous. Therefore, the water sorption characteristics of the ceramic will need to be characterized as an input parameter for modeling. Alternative materials such cerium oxide will also be considered.

→ To pressure system

Pressure transducer

Adapter

← To DAQ

Commercial pressure fittings

Small diameter, thick-walled tubing

Top fitting

K-type thermocouple

Plenum spring

Nichrome shim

Cladding

Stacked surrogate ceramic pellets

Bottom fitting

✹ = Spot weld

⊘ = Circumferential weld
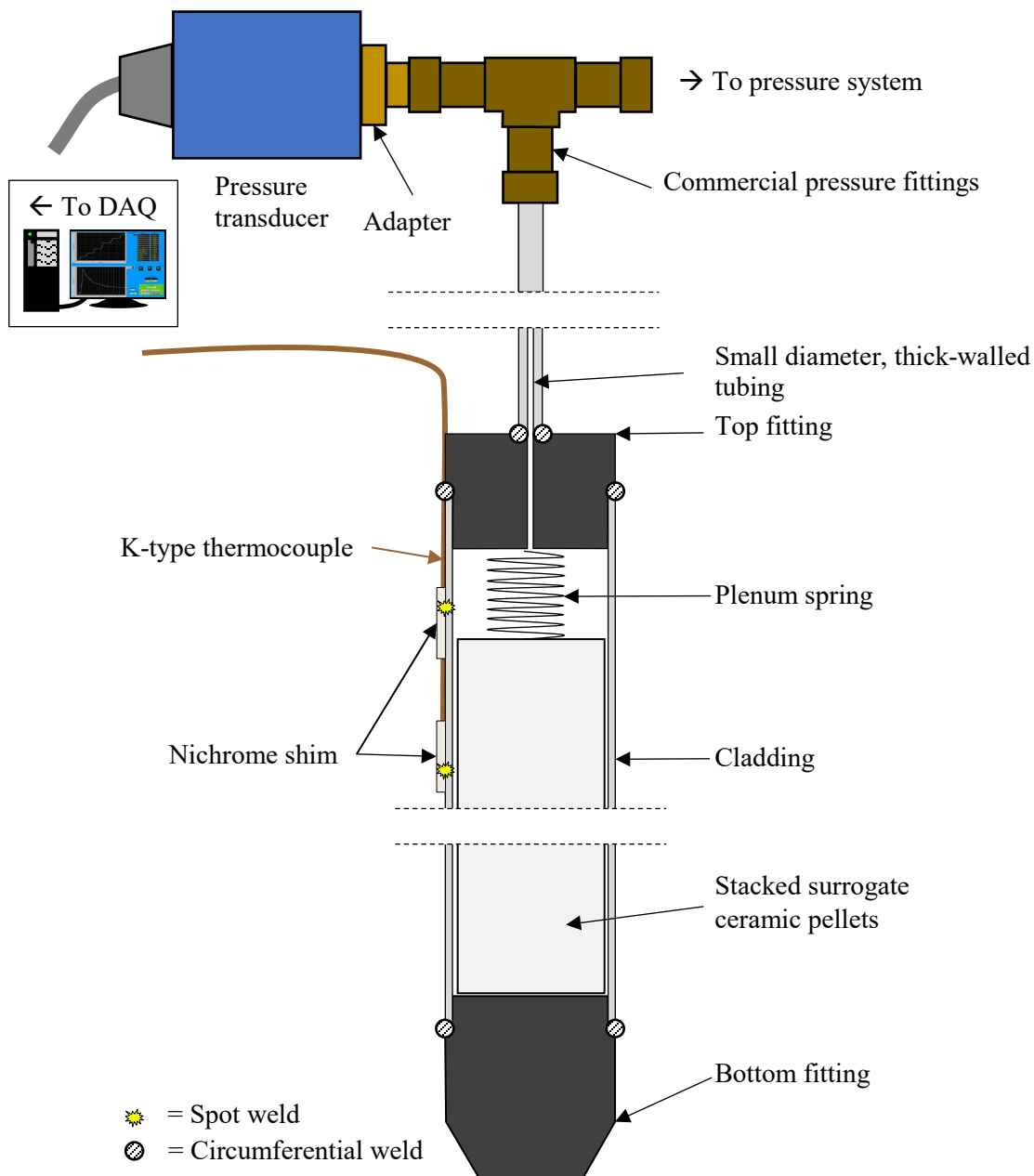
Figure 4.1   Cross-sectional view of pressure measurement rods
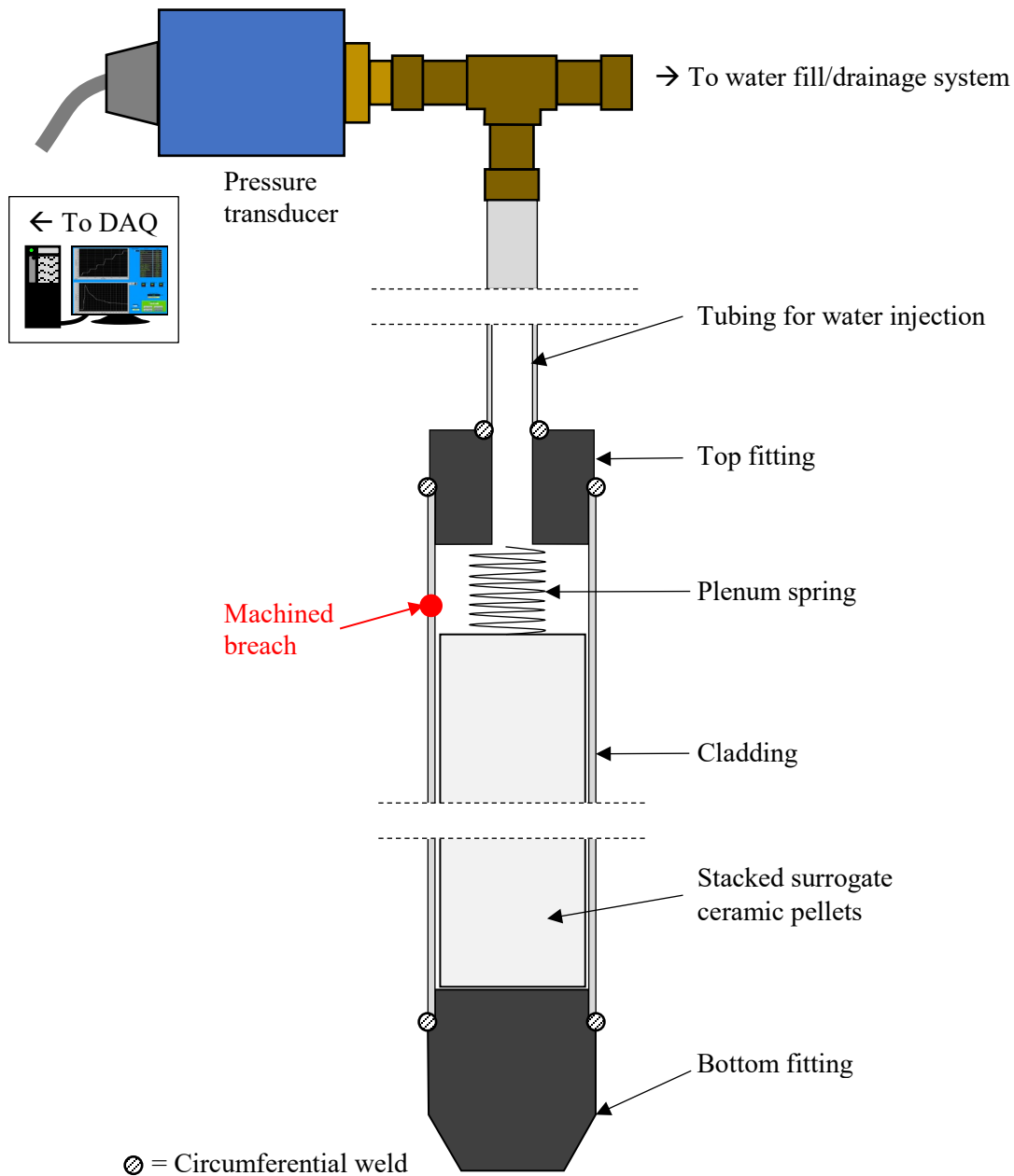
Figure 4.2   Cross-sectional view of breached cladding test concept.

4.4 Canister Drying Testing

4.4.1 Methodology

The advanced dry cask simulator will be used to experimentally simulate all the steps important to the commercial drying of a spent nuclear fuel canister. A highly prototypic electrically heated fuel assembly will be located inside of a pressure/vacuum vessel for this testing. Components that are known to complicate drying such as failed fuel rods or Boral neutron absorption plates will be incorporated. The test apparatus will be similar to the Dry Cask Simulator (DCS) that tested a single prototypic full length 9×9 BWR assembly in a 10" steel pipe pressure vessel. For the proposed drying study, the test assembly

will be either a single prototypic full length 17×17 PWR or a 3×3 array of 5×5 PWR subassemblies with a footprint of a single 17×17 PWR assembly. The PWR will be populated with newly developed waterproof heater rods so that the apparatus can be filled with water to submerge the bottom ~75% of the assembly.

The drying steps include purging out the water with dry helium and vacuum drying to below 3 torr, where pressures as low as 0.5 torr may be reached depending on the pump (Miller *et al.*, 2013). During this stage, the dew point of the vessel contents rapidly drops from a high value (perhaps 40 °C) to a low of -30 °C when the final pressure is reached. The volume fraction of water, however, rises rapidly from 7% in helium at a dew point of 40 °C to 100% as vaporizing water displaces the helium. Once the target vacuum is reached, the vacuum source is isolated from the vessel and the pressure rebound is measured for 30 minutes. If within that 30 minutes the pressure rises above 3 torr, the vacuum source is re-established, the vessel is evacuated back down to the target vacuum, and the rebound test is repeated. The pressure rise is ideally due to the vaporization of residual water trapped or adsorbed in small crevasses. However, the pressure rise could also be due to small air leaks in the vacuum system. Drying is considered complete once the pressure does not rebound above 3 torr in 30 minutes. At this point, the vessel is backfilled with helium and the resulting residual moisture content is monitored for any changes with time as the assembly reaches a steady-state temperature.

Pressurizing the vessel with dry helium will greatly reduce the concentration of moisture but leave the dew point unchanged. Table 4.1 shows the dew point and moisture concentration theoretically expected for three levels of vacuum drying: the minimum achievable dryness down to 0.3 torr, a medium dryness where the pressure rebounded to 1.5 torr, and the maximum moisture content case that rebounded to the maximum allowed 3.0 torr. The dew points range from -30 °C to -5 °C and the final moisture concentration range from 47 ppm_v to 494 ppm_v.

Table 4.1   Theoretical moisture content achieved by various levels of vacuum drying followed by pressurization with dry helium to 6000 torr (8 bar).

Case	Dew Point (°C)	P_{tot} (torr)	vol fraction (-)	ppm_v (-)
min	-30	0.3	1.00000	1000000
min	-30	6000	0.00005	47
mid	-13	1.5	1.000000	1000000
mid	-13	6000	0.00025	247
max	-5	3.0	1.00000	1000000
max	-5	6000	0.00049	494

The integral vacuum drying test presents a challenging set of conditions for moisture monitoring. Moisture monitoring is a vital component to the proposed study. A number of technologies have previously been used by others for monitoring moisture in the gas phase that provide an absolute moisture concentration measurement. The most common are capacity humidity sensors, chilled mirror hygrometers, and tunable diode laser (TDL) absorption spectroscopy.

There are two fundamental approaches to implement moisture monitoring. The first monitoring approach is *in situ* to the pressure vessel with the obvious advantage of providing measurements with the most relevance to the internal environment. However, the complexity of the experimental steps and the elevated temperatures and pressures render capacitive sensors and chilled mirrors impractical. The upper temperature limit of chilled mirror probes is 120 °C and for capacitive probes it is 200 °C. Neither can be submerged in water and the temperatures in the upper portions of the pressure vessel will likely exceed these limits. Optical access inside the pressure vessel is problematic for *in situ* implementation of TDL.

The second approach is extractive where a sample stream is removed from the test apparatus for analysis. This is a natural approach for the vacuum drying step. Since the temperature of the extracted sample stream can be controlled, any or all three of the monitoring methods can be used. However, as the extractive flow drops with increasing vacuum the representativeness of the measurements to the environment inside the pressure vessel will diminish. Additionally, TDL cannot be used below 10 torr so the system would need to be isolated during the final vacuum drying stage. After the vacuum extraction step, monitoring the moisture during the pressure rebound and after backfilling with helium is problematic. Extracting a representative sample during these steps may perturb the system in ways that may be difficult to quantify unless the sample flow is small.

4.4.2   Moisture Monitoring Instrumentation

4.4.2.1   Traditional Moisture Monitoring Technologies

A number of traditional moisture monitoring technologies were considered for use in this testing including dew point meters, solid state humidity probes and TDL spectroscopy. The ideal moisture measurement for the vacuum drying tests would provide a measurement inside of the pressure/vacuum vessel near the top (above the water fill elevation). The temperature in this region is expected to be between 150 °C and 300 °C. These temperatures are too high for dew point probes or solid-state humidity probes although the use in the vacuum line is appropriate. The pressure will range from 0.2 torr up to 6000 torr and the moisture concentration will range from pure steam down to 50 ppm_v (-30 °C dew point). The vacuum levels are too low for TDL to work through the entire vacuum drying process.

4.4.2.2   Mass Spectroscopy

Mass spectroscopy (MS) is a nontraditional method for measuring the relative moisture concentration in gas (i.e. ppm_v). In order to obtain an absolute moisture concentration (i.e. g/m^3) an absolute pressure measurement of the gas sampled is needed. In MS, a small sample stream (1 to 10 cm^3/min) is ionized and drawn into a vacuum chamber through a quadrupole filter that only allows passage of a selected single mass ion. Because MS draws such a small sample flow, no perturbation of the system is expected. However, adsorption and desorption of water on the small-bore stainless-steel or glass capillary sample tube can be an issue. Heating the sample lines and quadrupole minimizes the problem but it will still take several minutes of sample flow for equilibrium to be reached. For slowly changing transient operations expected in drying operation the anticipated lags are expected to be manageable.

The Hiden HPR 30, 200 amu, Wide Pressure Range gas sampling analysis system was chosen as the primary instrument for monitoring moisture throughout the entire drying process. This instrument features an automated inlet valving, gauging and control for operation over the range 0.20 torr – 6,000 torr (low range: 0.2 torr to 3.2 torr; medium range: 10 torr to 75 torr; high range: 760 torr to 6000 torr) as well as an integrated automated calibration gas inlet. The instrument is configured with a bakeout heater jacket option that allows continuous quadrupole operation at 150 °C to minimize moisture adsorption and optimize moisture analysis performance. The detection limit for moisture is 20 ppm_v (-55 °C dew point).

A major advantage of using mass spectrometry to monitoring moisture is that the method will provide a complete chemical analysis of the gas. Not only is the concentration of moisture measured but the concentrations of nitrogen, oxygen and argon provide a quantitative measurement of the amount of air that has leaked into the system. With a simultaneous measurement of both moisture and air the contribution of each to the pressure rebound during each vacuum drying step can be quantified. Furthermore, in anticipation of possibly monitoring the drying operation in a commercial canister, the instrument will provide a hydrogen concentration measurement as an indicator of radiolysis with a detection limit of 50 ppm_v, and krypton and xenon as an indicator of failed rods with detections limits in the low parts-per-billion range.

The mass spectrometer will be calibrated for moisture using a Michell DG2 two-stage dew point generator (-40 °C to +20 °C dew points). The calibrator uses a dry gas source such as ultra-high purity

helium and generates a split stream that is saturated with moisture at a controlled temperature mixed with the dry gas to generate a gas with a known dew point between -40 °C to +20 °C. The dew point of the calibration gas will be verified by passing through a Michell S8000 chilled mirror hygrometer that can provide precision measurements to -60 °C dew point. Calibration for the components of air of interest (N_2, O_2, Ar, Kr, and Xe) is implemented by sampling ambient air. If the ambient air is drawn through the Michell S8000 hygrometer, the dew point measurement can be used to provide a calibration point for ambient moisture.

A bench mount, remote sensor Michell Optidew 401 chilled mirror transmitter (-40 °C to +20 °C dew point at 23 °C ambient) will be used to monitor the moisture content of the vacuum exhaust stream during vacuum drying operations. The gas stream will be cooled to below 30 °C or 40 °C before reaching the sample probe. The layout of the instrumentation is shown in Figure 4.3.
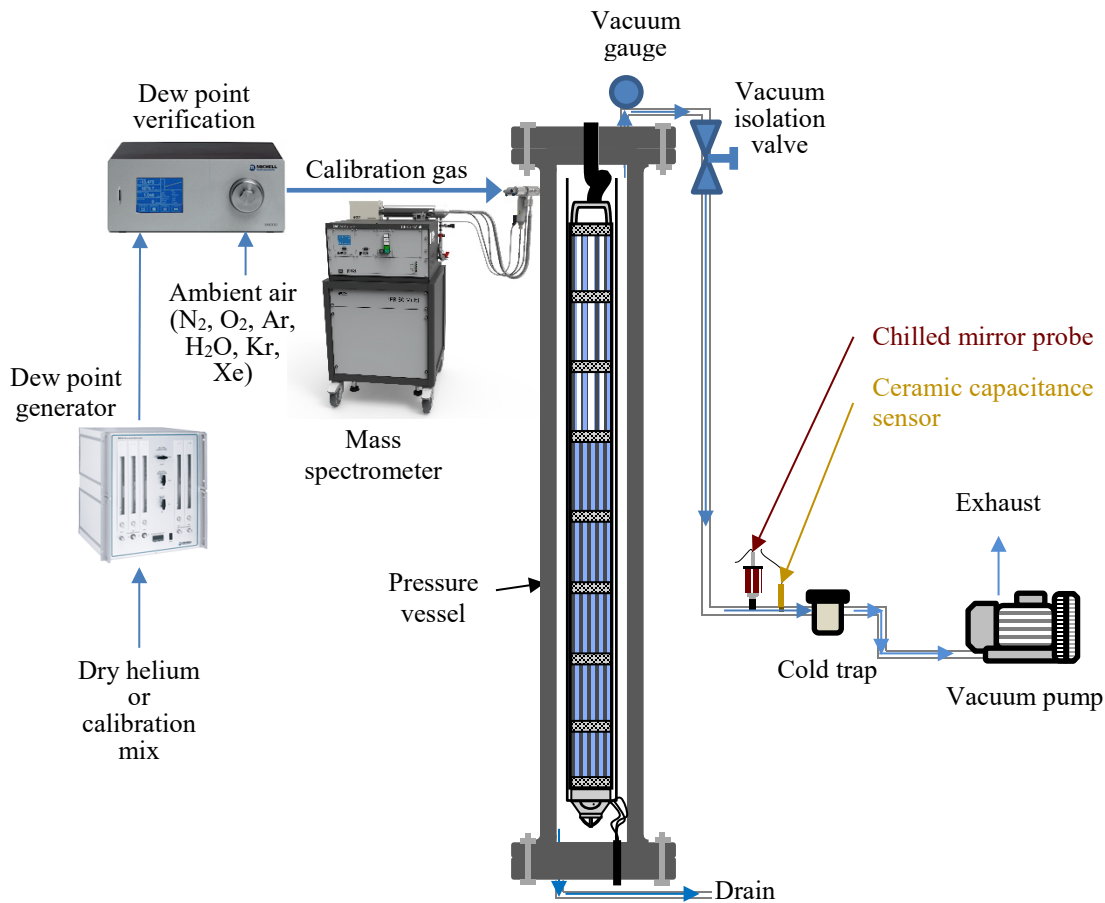
Figure 4.3   Moisture monitoring setup for canister drying testing.

4.5 Multi-Assembly Layout Components

Building on the success of the DCS (Durbin *et al.*, 2016), a multi-assembly test would bridge the prototypic complexity of the High Burnup Demo and the controlled environment of a lab-fielded apparatus. Several concepts have been explored and are the subject of ongoing research. One promising concept would use prototypic PWR skeletons to harvest "mini-assemblies" as shown in Figure 4.4. The mini-assemblies would retain prototypic geometric features but would be populated with waterproof, electrically resistive heaters and instrumentation. The fuel length would be prototypic and generate realistic temperature gradients, all while maintaining the intricate features of the guide tubes and grid spacers. Although the lateral extent of each assembly would be truncated, this configuration would

effectively incorporate heat transfer between assemblies as an improvement to the state of the art and offer a great deal of flexibility for future investigations.

The cross-sectionally truncated, full-length skeletons will be harvested from a 17×17 commercial skeleton. They will be comprised of 1 guide tube, 24 fuel pins, and all other fundamental hardware (top and bottom nozzles, spacers, intermediate flow mixers, debris catcher). Figure 4.5 shows the rearrangement of these assemblies in a basket structure inside a scaled dry storage canister. A truncated assembly with labeled dimensions is featured in Figure 4.6. The use of four obliquely-cut mini-assemblies with 21 fuel rods in the corners will allow for greater economy of space in the scaled system and more closely emulate the fraction of the fuel-occupied footprint in an actual cask.

The multi-assembly cask test will feature simplified, well-controlled boundary conditions and inputs. Multiple validation exercises will be possible with a versatile configuration. In this approach, pre-test modeling is tied with the experimental design, which features prototypic length and hardware. Multiple mini-assemblies will offer a key advantage in assessing inter-assembly interactions. Furthermore, the study intersects drying and cladding integrity research, allowing for a robust system performance assessment.

Figure 4.4   5×5 subassemblies taken from a 17×17 PWR skeleton

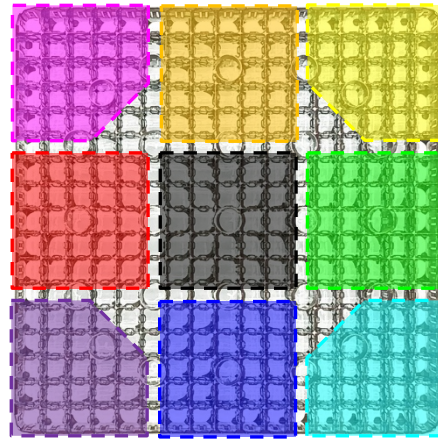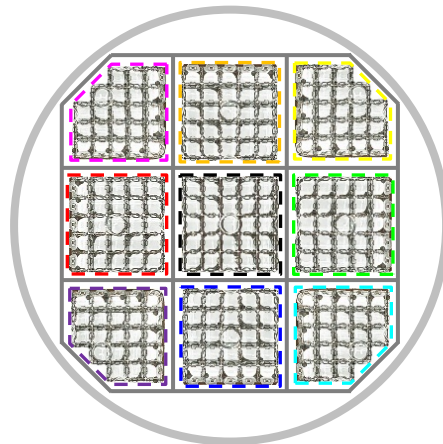**Figure 4.5   Reconfigured 5×5 mini-assemblies in a dry storage apparatus**
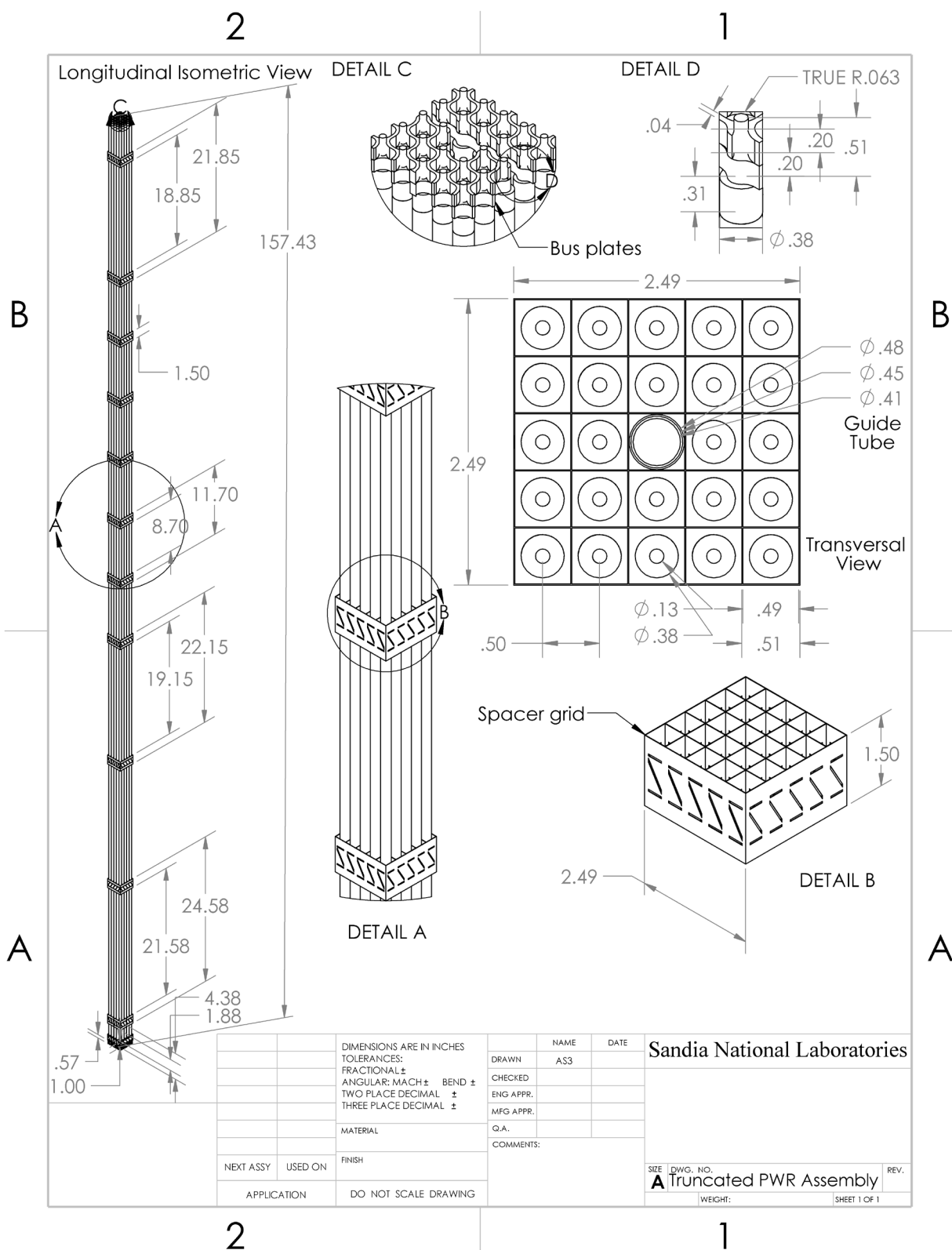
Figure 4.6   Schematic of truncated PWR assembly.

5 SUMMARY

Water removal from dry storage systems merits a detailed investigation due to a general lack of data and experience with the drying process. Validation of the extent of water removal in a dry storage system using an industrial vacuum drying procedure is needed, as operational conditions leading to incomplete drying may have potential impacts on the fuel, cladding, and other components in the system. Water remaining in casks upon completion of vacuum drying can lead to cladding corrosion, embrittlement, and breaching, and fuel degradation, so additional information is needed to evaluate the potential impacts of water retention on extended long-term dry storage. Smaller-scale tests that incorporate relevant physics and well-controlled boundary conditions are necessary to provide insight and guidance to the modeling of prototypic systems undergoing drying processes.

To date, Sandia National Laboratories has gained specialized experience from assembly-scale experiments and related sensor installation, air flow measurements, inert gas pressurization, and automated control. This practical experience has resulted in the proposal of future testing components for the study of spent fuel assemblies under drying and storage conditions. These specialized spent fuel rod simulators or surrogates are intended as building blocks for either truncated or full-scale, mock fuel assemblies. The proposed test apparatus would use these surrogates to measure the response of the fuel and the interior of the simulated dry cask system to well-controlled inputs and boundary conditions. The apparatus could provide temperature, pressure, and residual water data during wetting, drainage, blowdown, drying, and final backfill. Issues regarding bulk water retention and dryness criteria are of particular interest, and internal rod pressures could also be monitored to characterize fuel cladding during drying and storage.

The purpose of this report is to provide updates to the advanced components of this final test apparatus. Progress was made primarily on the development and testing of a waterproof heater rod. These tests focused on verifying the continuous operation of the heater rod under submersible conditions, exploring the feasibility and effectiveness of vacuum drying following water filling and the subsequent drainage and blowdown steps, and verifying the operation of the heater rod under backfill pressurization conditions. An upper-bound power level was chosen based on system temperature limitations, although this value was ultimately found to be too conservative.

The water filling and heating tests were carried out to demonstrate continuous operation of the waterproof heater rod under submersible conditions. Power outputs for this test were chosen such that the highest heater rod temperatures approached but did not exceed the local boiling point of water (94 °C) where water vapor could bridge the hot connection and the cladding and create a short. The consistent power output generated during this test, with no interruptions indicative of an electrical short, confirmed the ability of the current waterproof heater rod design to operate under submersible conditions at internal pressure vessel temperatures of up to 83 °C. The subsequent drainage and blowdown steps in this test demonstrated the effectiveness of these procedures in removing free water from the heater rod pressure vessel, and a mass balance confirmed a plausible amount of water remaining in the system. Future work will focus on bringing the highest temperatures of the test apparatus as close as possible to 94 °C through implementation of power feedback mechanisms. Subsequent tests may also involve potentially exceeding the 94 °C temperature limit to establish the parameters associated with heater rod failure. Temperature safety margins could be substantially increased if the Teflon insulators in the electrical feedthroughs are switched with Grafoil, which is rated to 495 °C.

The vacuum drying test was performed to verify waterproof heater rod performance in evacuated conditions and to demonstrate the effectiveness of applying vacuum in removing residual water from the pressure vessel following water drainage and blowdown steps. Measurement of pressure rebounds during vacuum holds in this drying test would be indicative of residual water removal from retention sites within the pressure vessel. The vacuum drying results recorded in this report are affected by the presence of a known, significant vacuum leak within the test apparatus, which necessitates further improvements in

order to properly assess the phenomenon of interest. Therefore, the accuracy of the results is limited and restricts the interpretation of these preliminary tests to a proof of concept. After correcting for the leak rate, the observed pressure increased during the system isolation. However, it remains inconclusive as to whether those pressure rebounds can be attributed strictly to residual water. Temperature increases during each evacuation and isolation/hold step were calculated to account for less than a 3 torr pressure increase.

Further testing must take place at steady-state temperature with a greater number of holds, and the gas drying equipment on the vacuum line should be employed to quantify the evacuated mass of water. It is also necessary to employ vacuum-regulating valves instead of full-vacuum for the procedure to be more prototypic. A pressure control system can be added to the vacuum line to maintain the pressure at the designated level of the hold within an acceptable margin of error. The use of vacuum-flanged pipes to construct the pressure vessel will result in greater leak tightness compared to common NPT pipes, and stronger vacuum pumps will allow for holds down to the ~0.1 torr scale, as the pump in this series was limited to the ~1 torr range.

The backfill tests were completed to demonstrate continuous operation of the waterproof heater rod under pressurized conditions in both helium and air. Helium tests were carried out at both 600 and 800 kPa, while an air test was carried out at 800 kPa. Continuous power output, with no interruptions indicative of a short, confirmed the ability of the current waterproof heater rod design to operate for up to 13 hours under 600 kPa helium and for up to 2 hours under both helium and air at 800 kPa. It was also confirmed that implementing a pressurized backfill improved heat transfer and reduced heater rod temperatures, and that helium may be used as a non-reactive gas in FHD drying tests that may substantially-reduce assembly temperatures in lieu of vacuum drying.

Future advanced concepts for dry storage cask thermal-hydraulic testing will involve implementing instrumentation for internal pressure monitoring and exploring the effects of breached cladding. Additional concepts to be explored will involve incorporating lessons learned from the waterproof heater rod tests into canister drying testing within a simulated dry storage cask, along with implementing moisture monitoring instrumentation within this simulated cask. The effects of cladding oxidation and crud on water retention in dry storage systems can also be explored via SETs, which would measure chemisorbed and physisorbed water content on cladding samples and provide data for incorporating these water retention properties either into cladding analogues or cladding with recreated oxidation and crud layers. These advanced concepts have the potential to be applied to a multi-assembly test that will bridge the prototypic complexity of the High Burnup Demo and the controlled environment of a lab-fielded apparatus.

6 REFERENCES

ASTM International (2016). Standard Guide for Drying Behavior of Spent Nuclear Fuel (C1553-16). ASTM Book of Standards Volume 12.01. West Conshohocken, PA.

Billone, M.C., Burtseva, T.A., & Han, Z. (2013). Embrittlement and DBTT of High-Burnup PWR Fuel Cladding Alloys (FCRD-UFD-2013-000401, ANL-13/16). Argonne National Laboratory. Lemont, IL.

Bryan, C. R., Jarek, R. L., Flores, C., & Leonard, E. (2019). Analysis of Gas Samples Taken from the High Burnup Demonstration Cask (SAND2019-2281). Sandia National Laboratories. Albuquerque, NM.

Chalasani, N., Araya, P. E., & Greiner, M. (2007). Simulations of Natural Convection/Radiation Heat Transfer for Horizontal and Vertical Arrays of Heated Rods Inside a Uniform Temperature Enclosure. 15th International Symposium on the Packaging and Transportation of Radioactive Materials. Miami, FL.

Csontos, A., Waldrop, K., Durbin, S., Hanson, B., Broussard, J., & Lenci, G. (2018). Spent Fuel Dry Cask Thermal Modeling Round Robin. European Nuclear Society Top Fuel Conference. Prague, Czech Republic.

Durbin, S. G., Lindgren, E. R., Humphries, L., Yuan, Z., Zavisca, M., Khatib-Rahbar, M., & Beaton, R. (2016). Spent Fuel Pool Project Phase II: Pre-Ignition and Ignition Testing of a 1x4 Commercial 17x17 Pressurized Water Reactor Spent Fuel Assemblies under Complete Loss of Coolant Accident Conditions (NUREG/CR-7216). NRC. Washington, D.C.

Greiner, M. (2017). Development and Experimental Benchmark of Simulations to Predict Used Nuclear Fuel Cladding Temperatures during Drying and Transfer Operations (NEUP 12-3660). University of Nevada, Reno.

Hanson, B.D. (2018). High Burnup Spent Fuel Data Project &Thermal Modeling and Analysis (PNNL-SA-13859). Nuclear Waste Technical Review Board Meeting. Albuquerque, NM.

Hanson, B.D., & Alsaed, H.A. (2019). Gap Analysis to Support Extended Storage and Transportation of Spent Nuclear Fuel: Five-Year Delta (SFWD-SFWST-2017-000005, Rev 1; PNNL-28711). Pacific Northwest National Laboratory. Richland, WA.

Knight, T. W. (2019). Experimental Determination and Modeling of Used Fuel Drying by Vacuum and Gas Circulation for Dry Cask Storage (NEUP 14-7730). University of South Carolina. Columbia, SC.

Knoll, R., & Gilbert, E. (1987). Evaluation of Cover Gas Impurities and their Effects on the Dry Storage of LWR (Light-Water Reactor) Spent Fuel (PNL-6365). Pacific Northwest National Laboratory. Richland, WA.

Lindgren, E. R., & Durbin, S. G. (2007). Characterization of Thermal-Hydraulic and Ignition Phenomena in Prototypic, Full-Length Boiling Water Reactor Spent Fuel Pool Assemblies after a Complete Loss-of-Coolant Accident (SAND2007-2270). Sandia National Laboratories. Albuquerque, NM.

Lindgren, E. R., Salazar, A., & Durbin, S. G. (2019). Component Concepts for Advanced Dry Storage Investigations (SAND2019-3587 R). Sandia National Laboratories. Albuquerque, NM.

Maharjan, D. (2018). Experimental Benchmark of Computational Fluid Dynamics Models to Predict Used Nuclear Fuel Cladding Temperatures during Vacuum Drying Conditions. PhD, University of Nevada, Reno.

Miller, L., Walter, G., Mintz, T., Wilt, T., & Oberson, G. (2013). Vacuum Drying Test Plan (NRC–02–07–C–006). CNWRA. San Antonio, TX.

Montgomery, R., Bevard, B., Morris, R. N., Goddard Jr., J., Smith, S. K., Hu, J., Beale, J., & Yoon, B. (2018). Sister Rod Nondestructive Examination Final Report (SWFD-SFWST-2017-000003 Rev. 1). Oak Ridge National Laboratory. Oak Ridge, TN.

Nakos, J. T. (2004). Uncertainty Analysis of Thermocouple Measurements Used in Normal and Abnormal Thermal Environmental Experiments at Sandia's Radiant Heat Facility and Lurance Canyon Burn Site (SAND2004-1023). Sandia National Laboratories. Albuquerque, NM.

Nuclear Regulatory Commission (2003). Spent Fuel Project Office Interim Staff Guidance-11, Revision 3. Washington, D.C.

Nuclear Regulatory Commission (2010). Standard Review Plan for Spent Fuel Dry Storage Systems at a General License Facility (NUREG-1536). Washington, D.C.

Scaglione, J.M., Montgomery, R.A., & Bevard, B.B. (2016). Post Irradiation Examination Plan for High Burnup Demonstration Project Sister Rods (FCRD-UFD-2016-000422; ORNL/SR-2016/111). Oak Ridge National Laboratory. Oak Ridge, TN.

Shalloo, M., Knight, T. W., Khan, J., Farouk, T., & Tulenko, J. (2017). Vacuum Drying Experiments Using a Mock Used Fuel Assembly. Trans. Am. Nucl. Soc., 117, 108-110.

APPENDIX A   DRAWINGS
A.1   Heater Rod Schematics

2   1

.38   .22   Line Connection

TRUE R.0625   .51   Threaded Portion

TRUE R.12   .70

TRUE R.27   End Cap

TRUE R.25

TRUE R.26   Ceramic Hermetic
                                                     Seal
TRUE R.2376

TRUE R.2166

B   Sheath   B

                                                     Heater Cladding

.70

1.45   44.54

                                                     Heating Element

                                                     Magnesium Oxide

                                                     End Plug
Plug Height   .75   Cold Pin
                                                     Well to Receive Cold Pin
Blind Hole Depth   .50
A   Chamfer   A
Pin Penetration Depth .375

45° Chamfer Height   .125

		DIMENSIONS ARE IN INCHES TOLERANCES: FRACTIONAL ± ANGULAR: MACH ± BEND ± TWO PLACE DECIMAL ± THREE PLACE DECIMAL ±		NAME	DATE	Sandia National Laboratories
			DRAWN	AS3		
			CHECKED			
			ENG APPR.			
			MFG APPR.			
		MATERIAL	Q.A.			
			COMMENTS:			
NEXT ASSY	USED ON	FINISH			SIZE DWG. NO. A Waterproof Heater Rod	REV.
	APPLICATION	DO NOT SCALE DRAWING			WEIGHT: SHEET 1 OF 8	

2   1
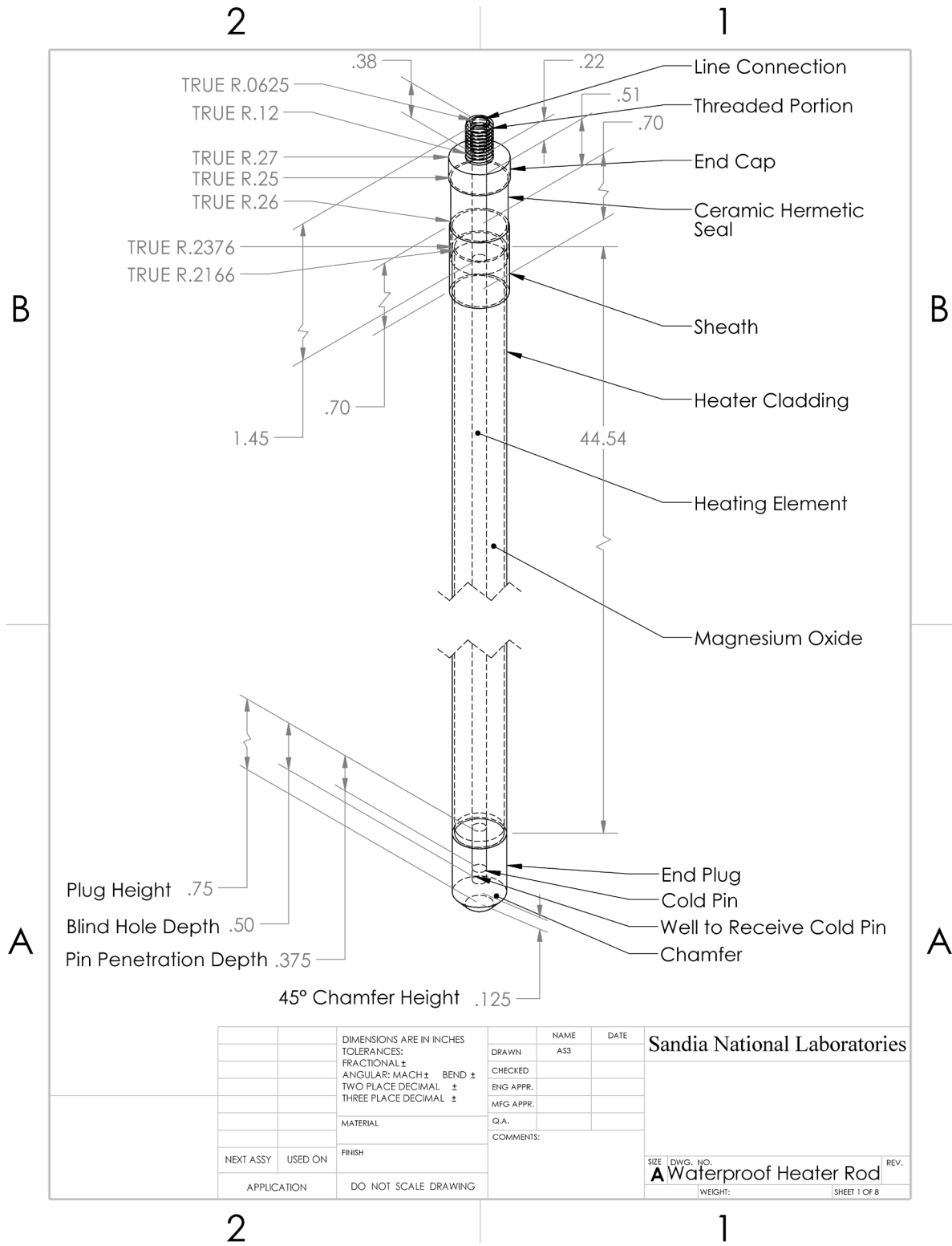
Figure A.1   Schematic of waterproof heater rod.

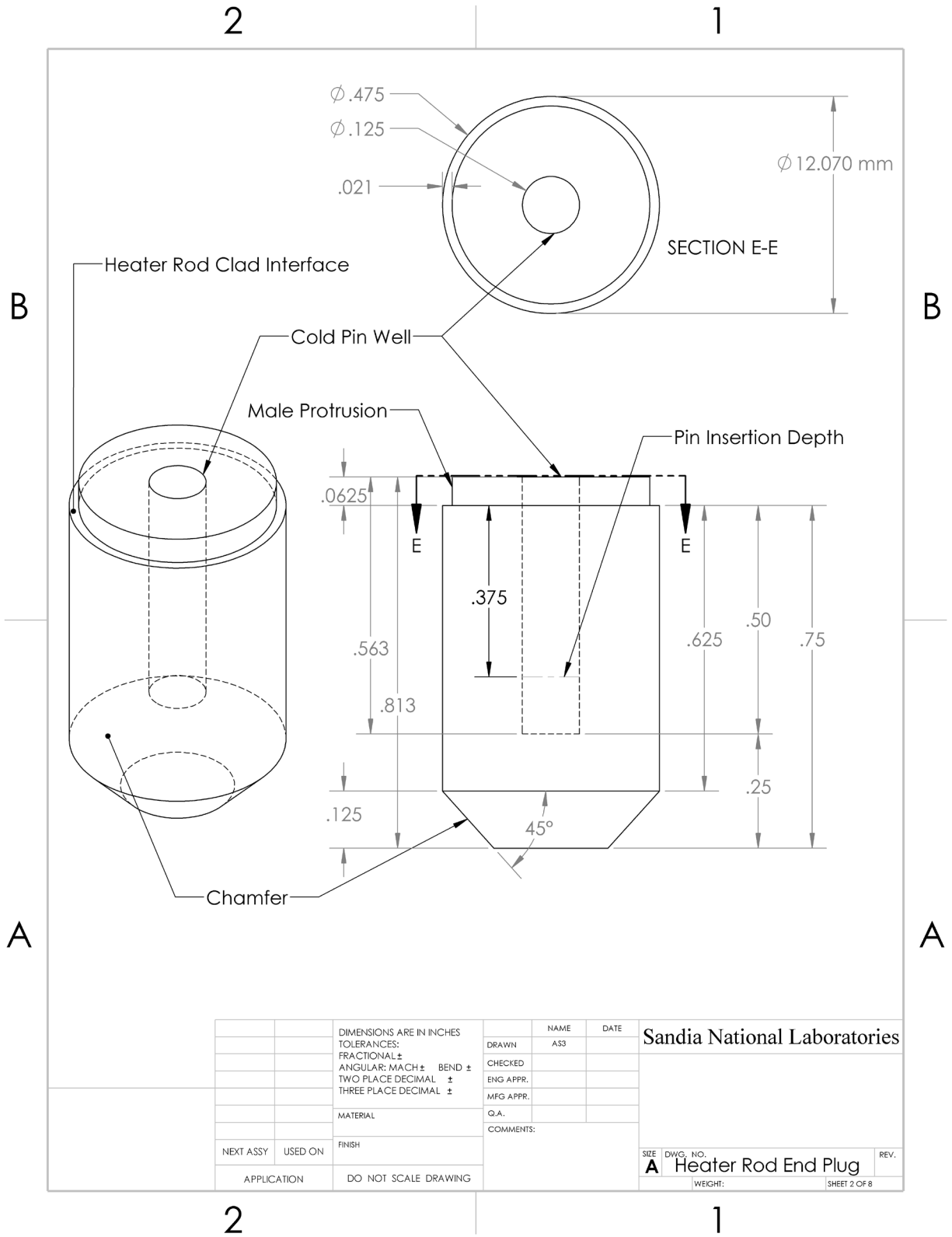**Figure A.2   Schematic of end plug.**

A.2   Pressure Vessel Details

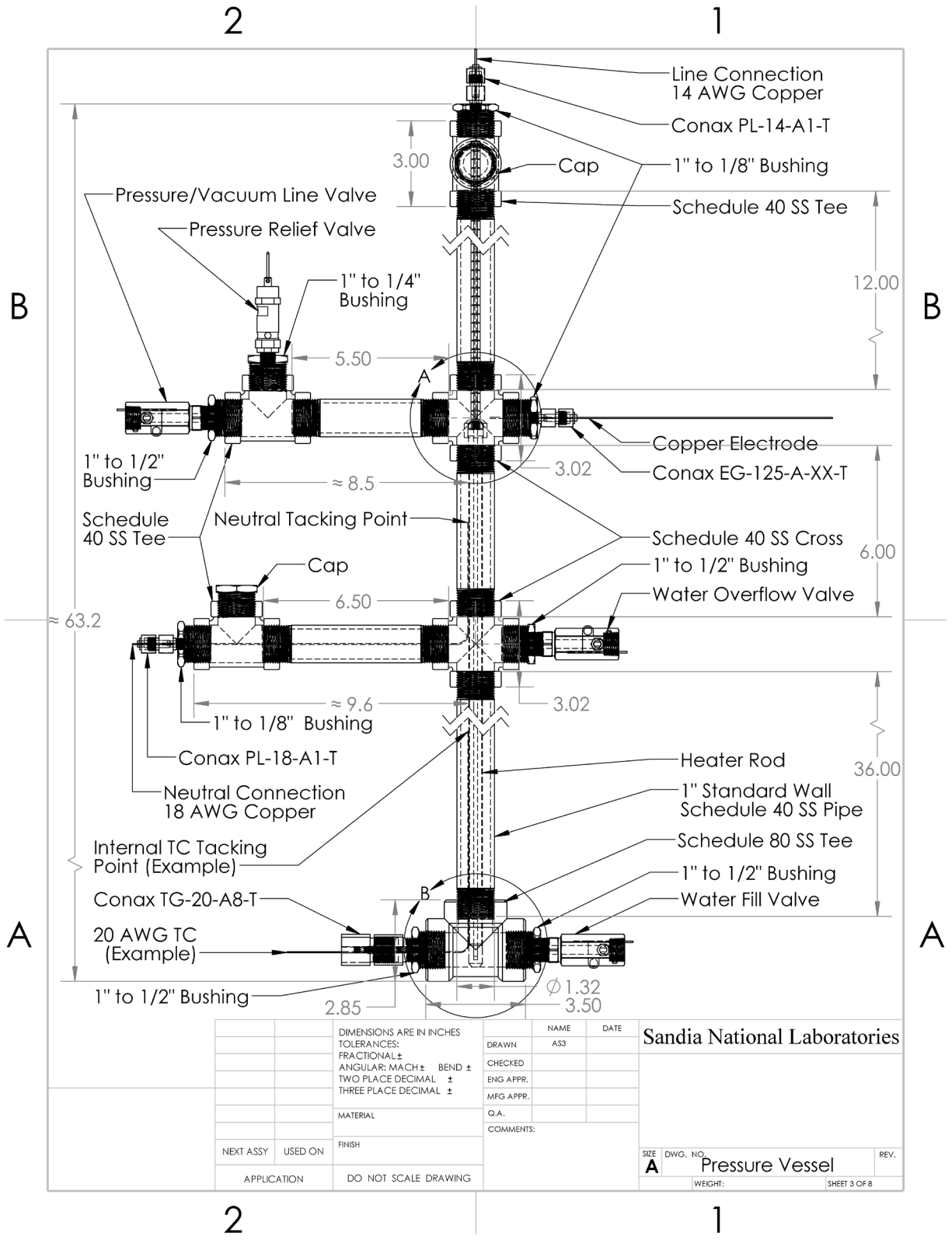**Figure A.3   Pressure vessel diagram with details A and B indicated.**

2   1

B   B

.35

TRUE ϕ .330

TRUE ϕ .133

Line Electrode 14 AWG

Non-Porous
High-Alumina
Ceramic Bead

Insulating Felt

Arc Threat Electrode

Hex Nut for Line
Connection Splice

(To Pressure Line)

Conax

Ceramic Hermetic Seal

Sheath

(To Bottom Tee)

DETAIL A

A   A

		DIMENSIONS ARE IN INCHES	NAME	DATE	Sandia National Laboratories		
		TOLERANCES:	DRAWN	AS3			
		FRACTIONAL±	CHECKED				
		ANGULAR: MACH± BEND ±	ENG APPR.				
		TWO PLACE DECIMAL ±					
		THREE PLACE DECIMAL ±	MFG APPR.				
		MATERIAL	Q.A.				
			COMMENTS:				
NEXT ASSY	USED ON	FINISH			SIZE **A**	DWG. NO. Top Cross	REV.
APPLICATION		DO NOT SCALE DRAWING			WEIGHT:		SHEET 4 OF 8

2   1
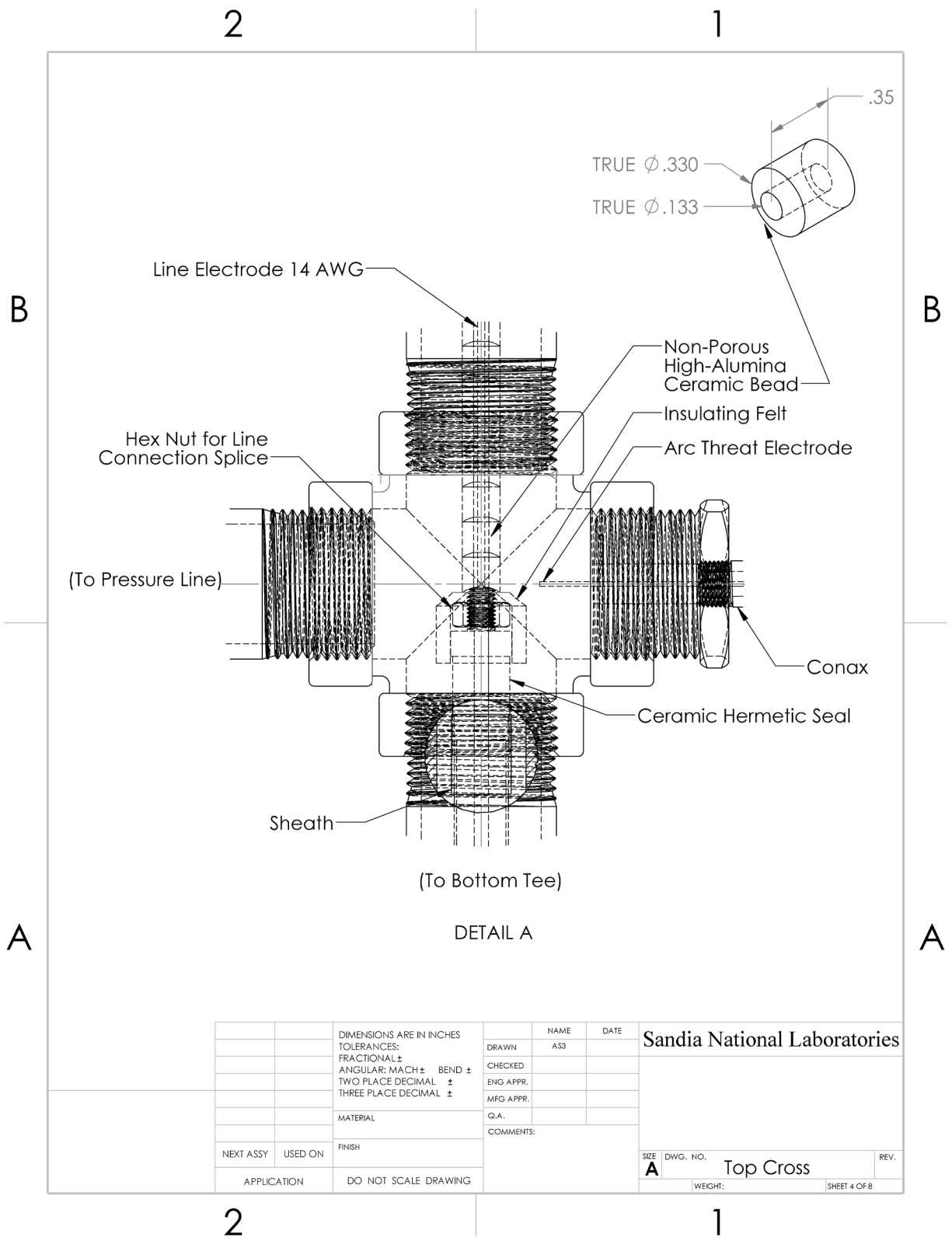
Figure A.4   Pressure vessel top cross detail shown with arc threat electrode for future testing.
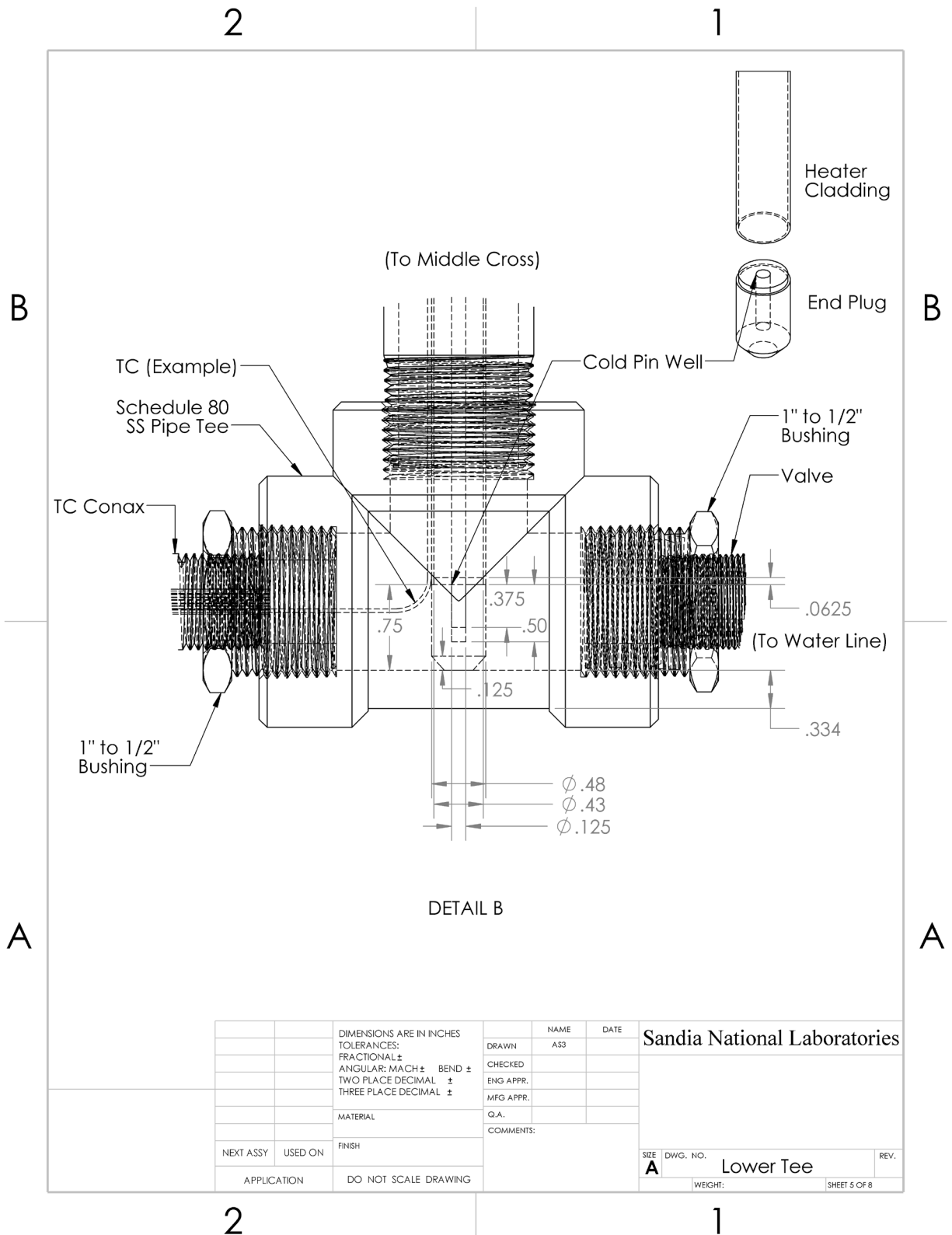
Figure A.5   Pressure vessel lower tee detail with one TC shown as an example.

This page is intentionally left blank.

APPENDIX B   PRESSURE SYSTEM

The pressure system is shown in Figure B.1. It is comprised of two gas lines: one dedicated to pressure (red) and the other to vacuum (green) and one water line (blue) interacting with the pressure vessel (black), where each line can be isolated with a valve. Pressure is applied to the stainless-steel vessel using a cylinder of air or inert gas (A1), where the flow rate and pressure are controlled by a reduced flow orifice (A3) and regulator (A4). Vacuum is applied using a vacuum pump (B1) with the specific pressure level set by a vacuum regulator (B2). Pressure levels are monitored by both regulator gauges (A4 and B2) and pressure transducers (A8 and B5) that are connected to a DAQ. Temperatures in the pressure vessel are monitored with axially-spaced thermocouples that also feed into the DAQ.

The pressure vessel consists of 1 inch 304 SS schedule 40 pipe joined by SS fittings D4 (sch. 40), D5 (sch. 40), and D6 (sch. 80) and 316 SS ball valves D1, D2, and D3. The schedule 40 components determine the MAWP of 1034 kPa (150 psi). A maximum pressure of 800 kPa (116 psi) will be applied to the system, and pressure under vacuum will not drop below 1 torr. The penetrants in the vessel include pressure and vacuum-rated Conax fittings that allow feedthroughs for the electrical line (L, at cross D4) and neutral (N, at cross D5) and thermocouples (at tee D6) that are connected to the DAQ. An arc challenge feedthrough is also present at cross D4 to investigate this effect when applying vacuum in future tests.

To reduce penetrants to the pressure vessel, the pressure and vacuum lines are united in the brown line, which provides a single connection to the ball valve D1. This ball valve is meant to isolate the pressure vessel from the pressure and vacuum lines and is normally open except during water fill operations when it is closed to protect those lines from bulk water flow. The ball valve D3 is used to allow for the filling and draining of water, and the ball valve D2 is an overflow valve meant to keep the water level below both the neutral weld between crosses D4 and D5 and the line connection in cross D4.

Water is introduced to the vessel using a transfer pump (C2), where the flow rate is controlled with a needle valve (C3) and rotameter (C4). The water level is controlled downstream with an overflow valve (D2) that leads to a drain (C9). Bulk water can be drained from the system via ball valve D3 either with gravity or by using gas from the pressure line in a blowdown (see purple line). A water container may be placed upstream of the drain to contain water for mass measurement.

The pressure line equipment is protected from backflows and water with a check valve (A9) rated for air, inert gas, and water. The vacuum line is ideally protected from water with a gas drying unit (B9) with silica desiccants, and a low-pressure relief valve (B11) set to 34 kPa (5 psi) protects the vacuum-rated PT (B5) from accidental pressurization. The vacuum-rated PT is redundantly protected by a solenoid isolation valve (B6) that is tripped by a pressure switch (B7, a relay transducer) at 34 kPa (5 psi). The water line equipment is protected from gas pressure with a check valve (C5) rated for air, inert gas, and water. The pressure line and pressure vessel are protected from overpressure with fast-acting PRVs (A7 and D7) set to 862 kPa (125 psi) with manual exhaust features. The PRV D7 is closest to the heater rod and has a temperature rating of 200 °C, while some feedthrough packing sets have a rating of 232 °C. Either of these limitations are addressed by using certain pipe lengths to increase separation from the heater rod.
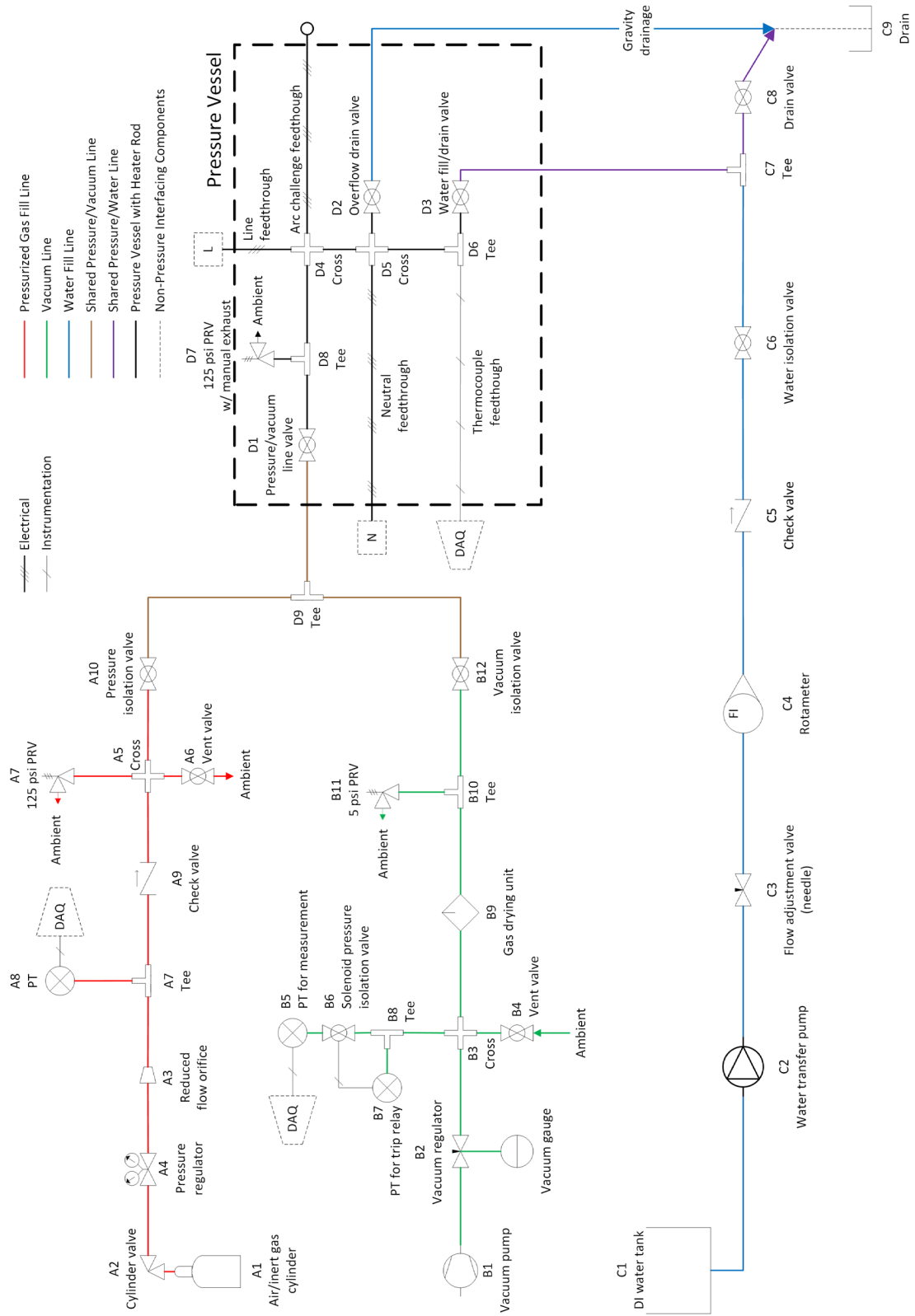
Figure B.1   Schematic of pressure system.